bioRxiv preprint doi: https://doi.org/10.1101/141820; this version posted May 24, 2017. The copyright holder for this preprint (which was not certified by peer review) is the author/funder, who has granted bioRxiv a license to display the preprint in perpetuity. It is made available under aCC-BY-ND 4.0 International license.

1 **Genetic Identification of a Common Collagen Disease in Puerto Ricans *via***
2 **Identity-by-Descent Mapping in a Health System**

3 G.M. Belbin[1,2,3], J. Odgis[2], E.P. Sorokin[4], M-C. Yee[5], S. Kohli[1], B.S. Glicksberg[2,3,6], C.R.
4 Gignoux[4], G.L. Wojcik[4], T. Van Vleck[1], J.M. Jeff[1], M. Linderman[2,3,†], C. Schurmann[1], D.
5 Ruderfer[7,8,9,††], X. Cai[2], A. Merkelson[1], A.E. Justice[10], K.L. Young[10], M Graff[10], K.E.
6 North[10], U. Peter[11,12], R. James[13], L. Hindorff[14], R. Kornreich[2], L. Edelmann[2], O.
7 Gottesman[1,†††], E.E.A. Stahl[1,3,6,7], J.H. Cho[1,2,15], R.J.F. Loos[1,16], E.P. Bottinger[1††††],
8 G.N. Nadkarni[1], N. S. Abul-Husn[1,2,3,†††], E.E. Kenny[1,2,3,9*]
9

10 [1] The Charles Bronfman Institute for Personalized Medicine, Icahn School of Medicine
11 at Mount Sinai, New York, NY, USA.
12 [2] Department of Genetics and Genomics, Icahn School of Medicine at Mount Sinai, New
13 York, NY, USA.
14 [3] The Icahn Institute of Genomics and Multiscale Biology, Icahn School of Medicine at
15 Mount Sinai, New York, NY, USA.
16 [4] Department of Genetics, Stanford University School of Medicine, Stanford, CA
17 [5] Carnegie Institution for Science, Department of Plant Biology, Stanford, CA.
18 [6] Harris Center for Precision Wellness, Icahn School of Medicine at Mt Sinai, New York,
19 NY, USA.
20 [7] Broad Institute, Cambridge, MA, USA.
21 [8] Division of Psychiatric Genomics, Icahn School of Medicine at Mt Sinai, New York, NY,
22 USA.

bioRxiv preprint doi: https://doi.org/10.1101/141820; this version posted May 24, 2017. The copyright holder for this preprint (which was not certified by peer review) is the author/funder, who has granted bioRxiv a license to display the preprint in perpetuity. It is made available under aCC-BY-ND 4.0 International license.

23 [9] Center for Statistical Genetics, Icahn School of Medicine at Mt Sinai, New York, NY,
24 USA.
25 [10] Department of Epidemiology, University of North Carolina at Chapel Hill, Chapel Hill,
26 NC, USA
27 [11] Public Health Sciences Division, Fred Hutchinson Cancer Research Center, Seattle,
28 WA, USA.
29 [12] Department of Epidemiology, University of Washington School of Public Health,
30 Seattle, WA, USA
31 [13] National Institute on Minority Health and Health Disparities, National Institutes of
32 Health, Bethesda, MD, USA
33 [14] National Human Genome Research Institute, National Institutes of Health, Bethesda,
34 MD, USA
35 [15] Division of Gastroenterology, Icahn School of Medicine at Mount Sinai, New York, NY
36 [16] The Mindich Child Health and Development Institute, Icahn School of Medicine at
37 Mount Sinai, New York, NY, USA.
38

39 [†] Present address: Department of Computer Science, Middlebury College, Middlebury,
40 VT, USA
41 [††] Present address: Departments of Medicine, Psychiatry and Biomedical Informatics,
42 Vanderbilt Genetics Institute, Vanderbilt University Medical Center, Nashville, TN, USA
43 [†††] Present address: Regeneron Pharmaceuticals, 777 Old Saw Mill River
44 Rd, Tarrytown, NY, USA
45 [††††]Present address: Berlin Institute of Health, Kapelle-Ufer 2, 10117 Berlin, Germany

bioRxiv preprint doi: https://doi.org/10.1101/141820; this version posted May 24, 2017. The copyright holder for this preprint (which was not certified by peer review) is the author/funder, who has granted bioRxiv a license to display the preprint in perpetuity. It is made available under aCC-BY-ND 4.0 International license.

46 *Correspondence to: eimear.kenny@mssm.edu

47

bioRxiv preprint doi: https://doi.org/10.1101/141820; this version posted May 24, 2017. The copyright holder for this preprint (which was not certified by peer review) is the author/funder, who has granted bioRxiv a license to display the preprint in perpetuity. It is made available under aCC-BY-ND 4.0 International license.

48 **Abstract**

49 Achieving confidence in the causality of a disease locus is a complex task that often
50 requires supporting data from both statistical genetics and clinical genomics. Here we
51 describe a combined approach to identify and characterize a genetic disorder that
52 leverages distantly related patients in a health system and population-scale mapping.
53 We utilize genomic data to uncover components of distant pedigrees, in the absence of
54 recorded pedigree information, in the multi-ethnic Bio*Me* biobank in New York City. By
55 linking to medical records, we discover a locus associated with genetic relatedness that
56 also underlies extreme short stature. We link the gene, *COL27A1*, with a little-known
57 genetic disease, previously thought to be rare and recessive. We demonstrate that
58 disease manifests in both heterozygotes and homozygotes, indicating a common
59 collagen disorder impacting up to 2% of individuals of Puerto Rican ancestry, leading to
60 a better understanding of the continuum of complex and Mendelian disease.

61 **Introduction**

62 During the past two decades major advances in deciphering the genetic basis of human
63 disease have resulted in thousands of disorders that are now understood at a genetic
64 level[1,2]. This progress has led to the integration of genomic sequencing in clinical care,
65 especially for the diagnosis of rare genetic disease[3,4], and clinical sequencing is
66 increasingly offered to patients with known or suspected genetic disorders. In the past
67 few years, large national and international efforts[5–7] have emerged to enable patients
68 and health systems to share knowledge of rare genetic disorders and improve genetic
69 testing, resulting in improved healthcare management and outcomes for patients. In

bioRxiv preprint doi: https://doi.org/10.1101/141820; this version posted May 24, 2017. The copyright holder for this preprint (which was not certified by peer review) is the author/funder, who has granted bioRxiv a license to display the preprint in perpetuity. It is made available under aCC-BY-ND 4.0 International license.

70 parallel, many large regional and national biobank efforts[8–10] are underway to enable
71 the broad integration of genomics in health systems for genetic identification of
72 disease[11]. Such efforts have recently revealed clinically actionable variants[11,12] and
73 genetic disorders segregating at higher frequencies in general patient populations than
74 previously suspected. The increased promulgation of genomics in health systems
75 represents an opportunity to improve diagnostic sensitivity for more precise therapeutic
76 intervention and better health outcomes[13].

77 Despite this progress, most genetic diseases are still under-diagnosed[14] or
78 misdiagnosed.[15–17] A number of barriers exist for wholesale genetic testing and
79 diagnoses, including incomplete standardized guidelines for interpreting genetic
80 evidence of disease[18], variable penetrance or expressivity of phenotype[19], and that the
81 causal variant may be missed or mis-assigned during testing[20]. The latter is a
82 particularly pernicious problem in non-European populations due to systematic biases in
83 large genomic and clinical databases[21,22]. These challenges have led several research
84 groups to attempt to genetically identify disease by examining patient health patterns
85 using data from the Electronic Health Record (EHR)[23,24]. EHRs contain comprehensive
86 information on medical care throughout a patient's life, including medications, medical
87 billing codes, physician notes and generated reports (i.e. pathologic, genetic and
88 radiologic reports). EHRs have been used to clinically characterize well-known genetic
89 disorders, but have been of limited success for the vast cadre of less-characterized or
90 unknown disorders[25].

91 The gold standard of genetic disorder diagnosis involves testing both patient and family
92 members to confirm Mendelian segregation of the suspected underlying pathogenic

bioRxiv preprint doi: https://doi.org/10.1101/141820; this version posted May 24, 2017. The copyright holder for this preprint (which was not certified by peer review) is the author/funder, who has granted bioRxiv a license to display the preprint in perpetuity. It is made available under aCC-BY-ND 4.0 International license.

93 variant[26–28]. However, as genomic data becomes more ubiquitous in health systems, it
94 can be used to detect genetic relationships in the absence of known family and
95 pedigree information. Specifically, components of pedigrees can be uncovered within
96 the general population; particularly those that have experienced recent founder effects.
97 Pairs of individuals who are related share genetic homology in the form of long genomic
98 haplotypes. These haplotypes are considered to be identical-by-descent (IBD) if they
99 are inherited from a common ancestor without any intervening recombination. The
100 chance of any two people sharing a tract of their genome IBD decays exponentially,
101 with a ~50% reduction in the chance of sharing per generation. However, when IBD
102 sharing does occur, the length of an IBD segment can remain long even between
103 distantly related individuals. In practice, long tracts of IBD (>3cM) can be accurately
104 detected using genetic data between individuals with a common ancestor from the past
105 4-50 generations[29]. Detection of IBD haplotypes can allow for the identification of
106 distantly related patients with a genetic disorder driven by a locus inherited from a
107 founding ancestor who brought the disease mutation into a population[30–37]. This is the
108 principle underlying population-scale disease mapping approaches that combine IBD
109 sharing and statistical association to discover novel disease loci, so called IBD-
110 mapping.

111 By detecting genetic relatedness, as inferred by IBD sharing, we hypothesized that we
112 may be able to detect hereditary forms of disease in an EHR-linked biobank. With over
113 38000 participants, the Bio*Me* biobank, at the Icahn School of Medicine at Mount Sinai,
114 New York City (NYC), is one of the most diverse cohorts ascertained at a single urban
115 medical center under a uniform study protocol. Participants are largely from the local

bioRxiv preprint doi: https://doi.org/10.1101/141820; this version posted May 24, 2017. The copyright holder for this preprint (which was not certified by peer review) is the author/funder, who has granted bioRxiv a license to display the preprint in perpetuity. It is made available under aCC-BY-ND 4.0 International license.

116 Upper East Side, Harlem and Bronx communities, and represent broad ancestral,
117 ethnic, cultural, and socioeconomic diversity. We initially focused on adult height, which
118 is easily measurable, stable over the adult life course, and one of the most abundantly
119 recorded clinical parameters in EHRs. Height is known to be highly heritable and
120 polygenic[38,39], however, extremes of short stature can be caused by rare variants in
121 single genes with large effect sizes[40]. Although, many genetic syndromes are known to
122 cause short stature, most of the time no definitive etiology underlying short stature is
123 found in patients. Here we used loci associated with genetic relatedness as measured
124 by IBD to map a locus underlying extreme short stature in the Bio*Me* biobank, and
125 linked it to a known, but little characterized, collagen disorder previously thought to be
126 rare. By interrogating a large global diversity panel, we demonstrated that this variant is
127 actually common in Puerto Rican populations. Furthermore, we leveraged the EHR to
128 show significant musculoskeletal disease in both heterozygous and homozygous
129 patients, indicating the disease is not simply a recessive disorder as had previously
130 been thought. Finally, we showed how this work can generate broad insights for
131 sustainable adoption and large-scale dissemination of genomic medicine.

132 Results

133 *Detecting Patterns of Diversity, Founder Effects and Relatedness in the BioMe Biobank*
134 *from New York City*

135 The Bio*Me* biobank comprises a highly diverse cohort, with over 65% of participants
136 self-reporting as Black/African-American or Hispanic/Latino, and over 35% born outside
137 mainland US, representing more than 110 countries of origin. First we estimated

bioRxiv preprint doi: https://doi.org/10.1101/141820; this version posted May 24, 2017. The copyright holder for this preprint (which was not certified by peer review) is the author/funder, who has granted bioRxiv a license to display the preprint in perpetuity. It is made available under aCC-BY-ND 4.0 International license.

138 patterns of direct relatedness in a subset of Bio*Me* participants genotyped on the
139 Illumina OmniExpress array (N=11212) by detecting pairwise identity-by-state using
140 RELATEAdmix[41], a method that accounts for admixture in populations (**Figure 1- figure**
141 **supplement 1**). We observed that 701 individuals had primary (parent-child, sibling) or
142 secondary (avuncular, grandparental) relationship with another participant in BioMe,
143 and we removed these individuals from all downstream analysis. Next we devised a
144 strategy to divide the diverse Bio*Me* biobank into population groups for downstream
145 analysis. We combined genotype data for Bio*Me* participants (N=10511) with 26 global
146 populations from the 1000 Genomes project (N=2504)[42] and two additional panels of
147 Native American (N=43)[43] and Ashkenazi Jewish populations (N=100) (see Methods).
148 Using a common set of 174468 SNPS we performed principal component analysis[44]
149 (PCA; **Figure 1 – figure supplement 2**). Based on both self-reporting and patterns of
150 genetic diversity observed in Bio*Me* participants, we stratified individuals into four broad
151 population groups. The first group self-reported as European American, but were also
152 genetically identified as Ashkenazi Jewish (AJ; N=808) as they clustered distinctly with
153 an AJ reference panel and separately from other European ancestry groups in PCA
154 space (**Figure 1- figure supplement 3**). The other three groups we defined using self-
155 reported race/ethnicity categories, African-American (AA; N=3080), Hispanic/Latino
156 (H/L; N=5102) and European-Americans with no AJ genetic ancestry (Non-AJ EA;
157 N=1270) (**Figure 1- figure supplement 3**). An additional 251 individuals who reported
158 'Mixed' (N=89) or 'Other' (N=162) ethnicity were excluded from further analysis.

159 To evaluate signatures of distant relatedness Bio*Me* biobank participants, we estimated
160 sharing of genomic tracts IBD >3cM between every pair of individuals using the

bioRxiv preprint doi: https://doi.org/10.1101/141820; this version posted May 24, 2017. The copyright holder for this preprint (which was not certified by peer review) is the author/funder, who has granted bioRxiv a license to display the preprint in perpetuity. It is made available under aCC-BY-ND 4.0 International license.

161 GERMLINE software[45]. The minimum length of 3cM was chosen based on reports of
162 elevated type I error in call rates of smaller lengths[46,47]. It is known that population-level
163 rates of distant relatedness are observed to be particularly elevated after population
164 bottlenecks (*i.e.* in founder populations)[48]. We summed the length of all IBD-tracts
165 shared between a given pair of individuals if they shared more than one tract and
166 examined the distribution of pairwise sharing at a population level. We observed
167 elevated levels of distant relatedness in both the AJ (median summed length of IBD
168 sharing within population=44.7cM; 95% C.I. = 44.66-44.82cM) and HL (16.2cM; 16.18-
169 16.22cM) populations, compared to AA (3.77cM; 3.76-3.77cM) or non-AJ EA (4.5cM;
170 4.45-4.55cM) populations (Figure 1A). This is congruent with previous reports of
171 founder effects in both AJ populations[49] and in some H/L populations[50].

172 Hispanic or Latina is a broad ethnic label encompassing myriad populations with origins
173 in Northern, Southern or Central America, century-long roots in New York City, and
174 genetic ancestry from Africa, Europe and the Americas. To explore the signature of a
175 founder effect in the Bio*Me* H/L population, we leveraged self-reported and genetic
176 information about sub-continental ancestry. By self-reporting, the H/L participants in
177 Bio*Me* were born in New York City (NYC) (40%), Puerto Rico (24%), Dominican
178 Republic (19%), Central/South America (12%), Mexico (2%) or other Caribbean Island
179 (2%) (**Figure 1B**). We examined IBD tract length distributions within H/L sub-
180 continental populations and observed that the founder effect was predominantly driven
181 in the Puerto Rican-born group (**Figure 1C**). We assembled a cohort of Puerto Ricans
182 including Bio*Me* participants who were either born in Puerto Rico or, were born in NYC
183 and had 2 parents or 3-4 grand parents who were born in Puerto Rico (N=1245).

bioRxiv preprint doi: https://doi.org/10.1101/141820; this version posted May 24, 2017. The copyright holder for this preprint (which was not certified by peer review) is the author/funder, who has granted bioRxiv a license to display the preprint in perpetuity. It is made available under aCC-BY-ND 4.0 International license.

184 Approximately 5086 NYC-born H/L individuals did not have recorded parental or
185 grandparental country-of-origin, therefore we also devised a selection strategy using
186 PCA analysis. We identified Bio*Me* H/L participants on the cline between the African
187 and European reference panels in PCA space coincident with Puerto Rican-born
188 individuals. We excluded those on the same cline with ancestry from the Dominican
189 Republic or another Caribbean Island **(Figure 1 – figure supplement 4),** and counted
190 the remainder (N=1571) in the Puerto Rican group. In total, we estimated 2816 H/L in
191 the BioMe discovery cohort were of Puerto Rican ancestry, and focused the
192 downstream analysis on this group as the largest founder population in Bio*Me*.

193 *Detecting a Locus Shared Identical-by-Descent Underlying Extreme Short Stature in*
194 *Puerto Ricans*

195 Next we tested the hypothesis that rare, recessive disease variants may have arisen to
196 appreciable frequency in the Puerto Rican founder population. We linked genomic data
197 to clinical data in the Electronic Health Record (EHR) of the Mount Sinai Health System.
198 We focused on height, a stable and ubiquitous health measure. Clinically, rare
199 instances of growth failure or 'short stature' may be caused by a large heterogeneous
200 group of genetic disorders (i.e. skeletal dysplasias)[51]. We first extracted measures of
201 height for the Puerto Rican adult population of Bio*Me* (mean age=55.3, standard
202 deviation (s.d.)=16.1). After making exclusions based on age (>= 18 years old for
203 women, >=22 years old for men, and < 80 years old in both sexes), mean height
204 measurements (mean height=5' 8.2", s.d.=3.2" for men; mean height=5' 2.8" s.d.=2.8"
205 for women) were consistent with those reported for Puerto Rican populations in a recent
206 global study on height[52]. We noted that 56 Puerto Ricans met the clinical definition of

bioRxiv preprint doi: https://doi.org/10.1101/141820; this version posted May 24, 2017. The copyright holder for this preprint (which was not certified by peer review) is the author/funder, who has granted bioRxiv a license to display the preprint in perpetuity. It is made available under aCC-BY-ND 4.0 International license.

207 short stature[53] (range of short stature 5'1"-4'0" in men, and 4'8"-3'8" in women) defined
208 as 2 standard deviations below the population-specific mean for men and women
209 separately (**Figure 2 – figure supplement 1**).

210 To test for recently arisen, recessive variants underlying clinical short stature in Puerto
211 Ricans, we implemented a previously published pipeline for 'IBD mapping'[31,54] (**Figure 2**
212 **– figure supplement 2**). We first clustered participants into 'cliques' of 3 or more
213 individuals whom, at a given genomic region, shared overlapping homologous IBD
214 tracts of at least 0.5cM in length. Membership in a clique indicates the sharing of a
215 recent common ancestor at that locus, from which the homologous IBD tract was jointly
216 inherited. Clustering of IBD into cliques in the Puerto Rican population (N=2816)
217 yielded 1434421 IBD-cliques after quality control filters (see methods). The site
218 frequency spectrum of IBD-cliques (**Figure 2 – figure supplement 3**) demonstrates an
219 expected exponential distribution of clique sizes (of 3-77 haplotypes), representing a
220 class of rare IBD haplotypic alleles (allelic frequency 0.0005-0.0137). To test whether
221 any cliques of IBD haplotypes were significantly associated with height we performed
222 genome-wide association of height as a continuous trait under a recessive model using
223 PLINKv1.9[55,56], including the first five PCA eigenvectors as covariates (see Methods).
224 We restricted analysis to homozygous IBD-haplotypes that were observed among at
225 least 3 individuals (480 cliques in total). Adjusting for 480 tests (Bonferonni adjusted
226 threshold $p<1x10^{-4}$) one IBD-clique achieved a genome-wide significant signal at the
227 locus 9q32 (IBD-clique frequency=0.012; β=-3.78; $p<2.57x10^{-11}$) (**Figure 3A**), spanning
228 a large mapping interval chr9:112MB-120MB. The clique contains 59 individuals, 56 of
229 whom are heterozygous and 3 are homozygous for the associated IBD haplotype.

bioRxiv preprint doi: https://doi.org/10.1101/141820; this version posted May 24, 2017. The copyright holder for this preprint (which was not certified by peer review) is the author/funder, who has granted bioRxiv a license to display the preprint in perpetuity. It is made available under aCC-BY-ND 4.0 International license.

230 *Fine-mapping Short Stature Locus Reveals Putative Link to Mendelian Syndrome*

231 The three individuals driving the recessive signal, two women and one man, were less
232 than 2.5 s.d. shorter (height reduction range 6”-10”) than the population mean for height
233 in the Puerto Rican cohort (**Figure 3B**). The IBD-haplotypes driving the signal spanned
234 a genic region with several candidate loci, and the minimum shared boundary
235 overlapped a single gene, *COL27A1,* which encodes for Collagen Type XXVII, Alpha 1
236 (**Figure 3C**). We performed whole genome sequencing (WGS) of the three homozygous
237 individuals, and an additional short-statured individual that we observed to possess a
238 homozygous IBD haplotype that was both directly upstream of and highly correlated
239 with the top IBD-clique. Individuals were sequenced to a depth of 4-18X coverage
240 (**Supplementary file 1**). Examination of variants that were observed in at least 6 copies
241 between the four individuals revealed a single candidate coding allele, a missense
242 mutation in Collagen Type XXVII, Alpha 1 (*COL27A1*, g.9:*116958257.C>G,*
243 NM_032888.1, p.G697R*,* rs140950220*)* (**Supplemental file 2**). *In silico* analysis
244 suggest that this glycine residue is highly conserved, and that a molecular alteration to
245 arginine at this position is predicted to be damaging (SIFT score=0.0; PhyloP
246 score=2.673; GERP NR score=5.67). These findings are consistent with a recent report
247 implicating the same *COL27A1* variant as causal for the rare orthopedic condition Steel
248 syndrome in a Puerto Rican family[57]**.** First described in 1993, the main clinical features
249 of Steel syndrome include short stature, bilateral hip and radial head dislocations, carpal
250 coalition (fusion of the carpal bones), scoliosis, *pes cavus* (high arches), and
251 dysmorphic features[58]**.**

bioRxiv preprint doi: https://doi.org/10.1101/141820; this version posted May 24, 2017. The copyright holder for this preprint (which was not certified by peer review) is the author/funder, who has granted bioRxiv a license to display the preprint in perpetuity. It is made available under aCC-BY-ND 4.0 International license.

252 To confirm the link between the IBD haplotype and the putative causal variant, we
253 calculated the concordance between the IBD haplotype and carrier status of the
254 *COL27A1*.pG697R variant by genotyping all of the homozygotes and carriers of the top
255 IBD-clique in the recessive model (N=59), along with a panel of age- and sex-matched
256 controls (N=59). This demonstrated 100% concordance between the *COL27A1*.pG697R
257 variant and the significant IBD-haplotype in homozygotes (**Supplementary file 3**). We
258 note that two Puerto Rican participants in the phase 3 1000 Genomes Project reference
259 panel (1KGP) were carriers of the *COL27A1*.pG697R variant, raising the possibility that
260 we may have been able to detect this association using more a traditional SNP
261 association approach. Therefore, we performed genome-wide association in the same
262 Puerto Rican cohort (N=2622) by first imputing the 1KGP panel and re-running the
263 recessive test as described above (n=10007795 imputed and genotyped SNPs with an
264 INFO score of > 0.3 and at least two observations of homozygotes). The recessive
265 model appeared to be well calibrated (λ=1.02), however, we observed no genome-wide
266 significant signal (**Figure 2 - figure supplement 4**). Association with the
267 *COL27A1*.pG697R variant was the 11775th most significant association (MAF=0.014:
268 β=-3.0; p<0.001). Upon examination of the correlation between the imputed
269 *COL27A1*.pG697R and the true carrier status of homozygotes, we noted a concordance
270 of only 66.67%, indicating that the IBD haplotype was a better tag of the true
271 *COL27A1*.pG697R homozygous state compared to 1KGP imputation in the Puerto
272 Rican cohort (**Supplemental file 3)**.
273
274 The association between *COL27A1*.pG697R and clinical short stature was replicated
275 using an independent cohort of 1775 individuals, from Bio*Me*, of self-reported Puerto

bioRxiv preprint doi: https://doi.org/10.1101/141820; this version posted May 24, 2017. The copyright holder for this preprint (which was not certified by peer review) is the author/funder, who has granted bioRxiv a license to display the preprint in perpetuity. It is made available under aCC-BY-ND 4.0 International license.

276 Rican ancestry, that were genotyped on the Illumina Infinium Multi-Ethnic Genotype
277 Array (MEGA) as part of the Polygeneic Architecture using Genomics and Epidemiology
278 (PAGE) Study. The *COL27A1*.pG697R (rs140950220) variant was directly genotyped
279 on MEGA, and an association of the variant under a recessive model resulted in a
280 strong signal of association (allele frequency=0.017; β=-3.5; s.e.=0.70; $p<4.87 \times 10^{-07}$).
281 The replication analysis revealed 51 additional Bio*Me* carriers and two individuals that
282 were homozygous for the variant. Both carrier and affected status was confirmed *via*
283 independent genotyping and Sanger sequencing (see Methods). The two homozygous
284 participants were both short statured (2.4 and 3.6 s.d from the sex specific population
285 mean).

286

287 *Evidence from Electronic Health Records Supports Suspected Cases of Steel*
288 *Syndrome*

289 To determine whether there was any clinical evidence to validate the link between the
290 *COL27A1*.pG697R variant and Steel syndrome, a clinical expert manually reviewed the
291 electronic health records (EHR), including clinical diagnoses, surgical procedures, and
292 radiology reports, of the five participants (3 women, 2 men, age range 34-74 years)
293 homozygous for the *COL27A1*.pG697R variant. Of note, there was no evidence that any
294 of the five patients had a clinical diagnosis of Steel syndrome. In all five individuals,
295 however, we found EHR-documented evidence of several previously described Steel
296 syndrome characteristics, including developmental dysplasia of the hip (or congenital
297 hip dysplasia), carpal coalition, scoliosis, and cervical spine anomalies (**Table 1**)[58,59]**.**
298 The incidence of cervical spine anomalies, including cord compression and spine

bioRxiv preprint doi: https://doi.org/10.1101/141820; this version posted May 24, 2017. The copyright holder for this preprint (which was not certified by peer review) is the author/funder, who has granted bioRxiv a license to display the preprint in perpetuity. It is made available under aCC-BY-ND 4.0 International license.

299 surgeries, was higher than previously reported (four out of five patients). There was also
300 evidence of other significant musculoskeletal complications, including lumbar and
301 thoracic spine anomalies in three patients, knee replacements in two patients (both
302 under age 50), and joint degeneration or arthritis in four patients. Together, these data
303 help further our understanding of Steel syndrome-associated characteristics and
304 potential complications that can occur later in life.

305 *Functional Investigation of COL27A1*.pG697R

306 To understand the biological mechanism underlying Steel syndrome, we investigated
307 the functional role of the *COL27A1* gene. *COL27A1* is a fibrillar collagen, which are a
308 class of collagens that contribute to the structural integrity of the extracellular matrix[60].
309 Enrichment of *COL27A1* RNA expression in vertebrae, as well as long bones, eyes, and
310 lungs has previously been observed in embryonic mice[60]. A mouse deletion of 87 amino
311 acids of the *COL27A1* homolog exhibited severe chondroplasia consistent with clinical
312 features observed in homozygotes[61], a similar musculoskeletal phenotype was
313 observed in knockdown of the *col27a1a* and *col27a1b* genes in zebrafish[62]. Type alpha-
314 1 collagen genes, of which *COL27A1* is a member, contain a conserved Gly-Xaa-Yaa
315 repeat in their triple helical domain[63]. Therefore, we hypothesized that the
316 *COL27A1*.pG697R variant may similarly disrupt stability of the *COL27A1* triple helix.

317 To test this hypothesis we modeled the effect of a glycine-to-arginine substitution in the
318 structure of a prototypical collagen peptide[64]. We observed that the glycine residues
319 occupied the center of the crowded triple helix, and that substitution for a bulkier
320 arginine would likely destabilize helix formation through steric hindrance (**Figure 2 –**

bioRxiv preprint doi: https://doi.org/10.1101/141820; this version posted May 24, 2017. The copyright holder for this preprint (which was not certified by peer review) is the author/funder, who has granted bioRxiv a license to display the preprint in perpetuity. It is made available under aCC-BY-ND 4.0 International license.

321 **figure supplement 5**). These data provide support for a functional model of the
322 pathogenicity of *COL27A1*.G697R through destabilization of the triple helix, which may
323 occur within developing spinal chords, long bones, and other tissues, resulting in the
324 observed clinical features in homozygotes. We note that many other collagen disorders,
325 including Ehlers-Danlos syndrome[65–67], Alport syndrome[68,69] and Osteogenesis
326 Imperfecta[70,71], are driven by molecular alterations of a glycine in the triple helix of the
327 underlying collagen genes. However, all of these disorders are inherited under an
328 autosomal dominant mode, in contrast to Steel syndrome, which has only been reported
329 as a recessive disease. This analysis raises the question of whether some and/or milder
330 clinical features of Steel syndrome may be present in carriers.

331 *Assessing the Health Records of COL27A1.pG697R Carriers Reveals Evidence of*
332 *Musculoskeletal Disease*

333 To test for clinical features of Steel syndrome in *COL27A1*.pG697R carriers, we
334 performed two analyses using EHR data. The first was a test for associated medical
335 billing codes (ICD9s) with *COL27A1*.pG697R carrier status, or Phenome-Wide
336 Association Study (PheWAS)[72,73]. PheWAS analysis is often performed using a general
337 linear model (GLM), however standard implementations often do not account for
338 scenarios where there is a large imbalance between per-test number of cases and
339 controls, rare variants/ICD9s or the presence of elevated distant relatedness. Therefore,
340 in addition to the GLM, we also ran three other score based tests; (i) that use
341 saddlepoint approximation (SPATest)[74] to account for case:control imbalance; (ii) a
342 linear mixed model (GCTA)[75] to account for distant relatedness; and (iii) a test that

bioRxiv preprint doi: https://doi.org/10.1101/141820; this version posted May 24, 2017. The copyright holder for this preprint (which was not certified by peer review) is the author/funder, who has granted bioRxiv a license to display the preprint in perpetuity. It is made available under aCC-BY-ND 4.0 International license.

343 incorporates a bias-reduction for small numbers of observations (Firth test)[76]. Each test
344 was run using ICD9 codes in all individuals of Puerto Rican ancestry (N=106
345 *COL27A1*.pG697R carriers and N=4480 non-carriers). The ICD9 code was set as the
346 outcome variable and *COL27A1*.pG697R as the primary predictor variable, including
347 age, sex and the first five PCAs as covariates in all tests. To avoid spurious
348 associations, we restricted the analysis to diagnosis codes with at least 3 observations
349 (n=367 ICD9 codes) amongst carriers.

350 Results of the GLM test are shown in **Figure 3** and **Table 2**. Of the five significantly
351 associated ICD9 codes (False Discovery Rate (FDR)<0.05), three involved the
352 musculoskeletal system 730.08 ($p_{GLM}<7.1x10^{-6}$; odds ratio (OR)=34.5; 95% Confidence
353 Interval (CI)=7.4-162), 721.0 ($p_{GLM}<6.6x10^{-5}$; OR=5.4; CI=2.4-12.3), and 716.98
354 ($p_{GLM}<4.4x10^{-4}$; OR=5.8; CI=2.2-15.3). ICD9 730.08 encodes for "acute osteomyelitis,
355 other specified sites". Manual review of chart records for these patients revealed that
356 this code referred to vertebral osteomyelitis in the three carriers with the ICD9 code.
357 ICD9 721.0 encodes for cervical spondylosis without myelopathy. Cervical spondylosis
358 refers to degenerative changes of the cervical spine, which can eventually progress to
359 encroach on the cervical canal, causing myelopathy (spinal cord injury). A third
360 diagnosis code, 716.98, encodes for "arthropathy, unspecified, or involving other
361 specified sites". Manual review of chart records for these patients revealed that this
362 code referred to knee arthropathy in all four patients. Finally, two other ICD9 codes
363 were significantly associated with the *COL27A1*.pG697R variant; 622.10 ($p_{GLM}<1x10^{-4}$;
364 OR=5.4; CI=2.3-12.6), which encodes for cervical dysplasia, and 789.1 ($p_{GLM}<2.1x10^{-4}$;
365 OR=11.6; CI=3.2-42.2), which encodes for hepatomegaly. Presently, it is unclear

bioRxiv preprint doi: https://doi.org/10.1101/141820; this version posted May 24, 2017. The copyright holder for this preprint (which was not certified by peer review) is the author/funder, who has granted bioRxiv a license to display the preprint in perpetuity. It is made available under aCC-BY-ND 4.0 International license.

366 whether these two are related to a *COL27A1*.pG697R carrier phenotype, or are
367 spurious associations.

368 We observed over inflation in the distribution of the PheWAS test statistic, measured by
369 lambda (λ), for all four score based models (λ_{GLM}=1.59; $\lambda_{SPATest}$=1.20; λ_{GCTA}=1.36;
370 λ_{Firth}=2.09), indicating that no single model fully accounts for the confounding effects of
371 distant relatedness, case:control imbalance and rare variants/ICD9s (**Figure 3 – figure**
372 **supplement 1**). The code linked to vertebral osteomyelitis (730.08) was the top signal
373 in all tests ($p_{SPATest}<1.4\times10^{-4}$; $p_{GCTA}<7.9\times10^{-10}$; $p_{Firth}<1.5\times10^{-9}$), but only remains
374 significant after genomic control adjustment in one of the tests ($p_{GCTA_adjusted}<4.6\times10^{-5}$).
375 Neither codes linked to cervical spondylosis (721.0; $p_{SPATest}<3.0\times10^{-3}$ (rank=3rd);
376 $p_{GCTA}<3.3\times10^{-3}$ (8th)) or knee arthropathy (716.98; $p_{SPATest}<0.022$ (21st); $p_{GCTA}<3.5\times10^{-3}$
377 (9th); $p_{Firth}<0.001$ (35th))) were significant after genomic control correction. Therefore,
378 while PheWAS analysis provided preliminary support of Steel syndrome-associated
379 clinical features in carriers, best practices for PheWAS models for rare variants/ICD9
380 codes, and in the presence of population structure, remains an open problem for the
381 genomics community. It is also possible that some relevant clinical features of Steel
382 syndrome might be poorly captured by or absent from medical billing codes.

383 To evaluate the preliminary evidence from the PheWAS analysis, we performed a
384 second analysis of EHR data that focused on a comprehensive manual chart review to
385 examine for evidence of Steel syndrome characteristics in the *COL27A1*.pG697R
386 carriers in the same manner as performed for homozygotes. We limited the analysis to
387 carriers below the age of 55 (N=34; mean age 41.8 years) to reduce confounding from

bioRxiv preprint doi: https://doi.org/10.1101/141820; this version posted May 24, 2017. The copyright holder for this preprint (which was not certified by peer review) is the author/funder, who has granted bioRxiv a license to display the preprint in perpetuity. It is made available under aCC-BY-ND 4.0 International license.

388 age-related related symptoms of spine and joint pain. We also selected 31 age and sex
389 matched Puerto Rican non-carriers for comparison (mean age 40.6 years). Utilizing the
390 same criteria used to characterize Steel syndrome cases, we found no evidence of
391 clinical short stature or hip dislocation in carriers, but did observe a trend of elevated
392 rates of major joint and spine degradation (**Table 1**). In general, 38% (13/34) of carriers
393 showed evidence of spine degeneration varied from severe (multiple level cord
394 compression and neurological symptoms necessitating corrective surgery) to moderate
395 (lower back pain with no neurological symptoms managed with physical therapy and/or
396 pain medication) compared to 13% (4/31) of non-carriers (Fishers exact test $p<0.03$).
397 Specifically, we found an increased risk of cervical stenosis in 15% (5/34) of carriers
398 compared to 0% (0/31) of controls ($p<0.05$). Although not reaching statistically
399 significance, we show a trend of 2-fold higher rates of scoliosis (24%; $p<0.35$), arthritis
400 (38%; $p<0.1$), and lumbar spine degradation (29%; $p<0.25$) in carriers compared to non-
401 carriers and previous published reports in similar age groups[77,78]. Together these data
402 suggest an appreciable burden of joint and spine degradation in *COL27A1*.pG697R
403 carriers (**Table 1**).

404 *Worldwide Frequency and Demographic History of COL27A1.pG69R*

405 Having genetically identified and clinically characterized a previously little-known
406 disease variant, we next investigated which populations were at risk for harboring the
407 allele. We assessed the carrier frequencies of the *COL27A1*.pG697R variant in global
408 panel of 51745 individuals from Africa (N=376), the Americas (N=45685), Asia
409 (N=5311), Europe (N=209), the Middle East (N=163) and Oceania (N=28) genotyped on

bioRxiv preprint doi: https://doi.org/10.1101/141820; this version posted May 24, 2017. The copyright holder for this preprint (which was not certified by peer review) is the author/funder, who has granted bioRxiv a license to display the preprint in perpetuity. It is made available under aCC-BY-ND 4.0 International license.

410 MEGA in the PAGE Study. This included; 13050 in the Multi-Ethnic Cohort (MEC)[79]
411 Study; 12327 in the Hispanic Community Health Study/Study of Latinos (HCHS/SOL)[80];
412 12852 in the Women's Health Initiative (WHI) Study[81]; 13044 additional Bio*Me* biobank
413 participants (including the 1775 Puerto Ricans on MEGA described above); and a
414 Global Reference Panel from Stanford University including the Human Genome
415 Diversity Panel[82] (N=986, see Methods). Combined, the PAGE and Bio*Me* dataset
416 represented 57316 individuals from 112 global populations (**Supplementary file 4**). The
417 *COL27A1*.pG697R C allele was present in 183 copies (173 heterozygous carriers and 5
418 homozygous cases). We estimate the carrier rate of *COL27A1*.G697R to be 1:51 in
419 Puerto Rican-born individuals (minor allele frequency (MAF)=1.1%); 1:9 in individuals
420 born on the island of St. Thomas (MAF=11%); 1:346 in Hispanic/Latinos in the US
421 (MAF=0.29%) and 1:72 in Bio*Me* Hispanic/Latino populations from New York City
422 (MAF=0.7%); and 1:746 in individuals born in the Dominican Republic (MAF=0.067%)
423 (**Figure 4A)**. We note that only 9 people were assayed from St. Thomas, so the high
424 carrier frequency estimate could be biased by small sample size. Finally, the variant is
425 present in only 4 copies in the 60,706 exomes in the ExAC database[83], likely due to
426 differences in the populations comprising both datasets.

427 To predict what other populations might be at risk for Steel syndrome, we explored the
428 locus-specific demographic history in carriers of the *COL27A1*.pG697R risk haplotype.
429 First, by visual inspection, we were able to discriminate a single haplotype of 107.5kb in
430 length that contained 55 SNPs, which uniquely tagged the *COL27A1*.pG697R variant
431 (R^2=1). This haplotype was present only in individuals born in Puerto Rico (N=25), the
432 Dominican Republic, (N=2), Columbia (N=1), New York City (N=40) and St. Thomas

bioRxiv preprint doi: https://doi.org/10.1101/141820; this version posted May 24, 2017. The copyright holder for this preprint (which was not certified by peer review) is the author/funder, who has granted bioRxiv a license to display the preprint in perpetuity. It is made available under aCC-BY-ND 4.0 International license.

433 (N=1). Genotyping determined that only the haplotype carriers from Puerto Rico, New
434 York City and St. Thomas also carried the *COL27A1*.pG697R variant (N=56 in total).
435 Second, we inferred continental ancestry along the genomes of the three Puerto Rican
436 homozygotes in the discovery cohort. Local ancestry inference is the task of assigning
437 continental ancestry to genomic segments in an individual with recent ancestors from
438 multiple continents. For the Puerto Rican homozygotes, we estimated local haplotypic
439 similarity with a reference panel of African, European and Native American genomes
440 using RFMix[84]. Examination of local ancestry on the background of the IBD haplotype in
441 all three homozygous individuals revealed all to be homozygous for Native American
442 ancestry, suggesting the *COL27A1*.pG697R arose on a Native American haplotype
443 (**Figure 4B**).

444 To test whether the disease variant arose via genetic drift or selection, we used the
445 IBDNe software[85] to estimate the historical effective population size (N_e) of the Puerto
446 Rican discovery cohort (N=2816) (**Figure 4C**). The IBDNe software calculates the
447 effective population size of a given population over past generations by modeling the
448 distribution of IBD tract lengths present in the contemporary population. The analysis
449 suggested evidence of a strong bottleneck in Puerto Ricans approximately 9-14
450 generations ago, with the smallest effective population sized dating approximately 12
451 generations ago (estimated N_e=2580, 95% C.I 2320-2910). This is consistent with the
452 timing of European immigration and slave trading on the Island, resulting in admixture
453 and population bottlenecking, followed by demographic growth post-contact[50,86]. Finally,
454 to see if there was evidence that the locus had undergone a recent selective sweep we
455 calculated the integrated haplotype score (iHS)[87,88] across chromosome 9 in phased

bioRxiv preprint doi: https://doi.org/10.1101/141820; this version posted May 24, 2017. The copyright holder for this preprint (which was not certified by peer review) is the author/funder, who has granted bioRxiv a license to display the preprint in perpetuity. It is made available under aCC-BY-ND 4.0 International license.

456 genotype data for Bio*Me* Puerto Rican samples, but did not observe evidence of
457 selection at the locus (**Figure 4 – figure supplement 1**). Together, this evidence
458 suggests that the *COL27A1*.pG697R variant arose in the ancestral Native American
459 populations that peopled the Caribbean, which underwent a strong bottleneck during the
460 period of colonization, which may help explain the prevalence of this disease in
461 amongst contemporary Puerto Rican populations.

462 **Discussion**

463 Here we describe a new approach to utilize genomic data in health systems for
464 identifying and characterizing genetic disorders, the cornerstone of which is the ability to
465 identify related individuals in the absence of recorded pedigree or genealogy
466 information. By linking medical records of distantly related patients, identified by shared
467 tracts of genetic homology identical-by-descent (IBD), we discovered a recessive
468 haplotype on 9q32 conferring extreme short stature. Whole genome sequencing
469 revealed that a mutation (Gly697Arg) in the *COL27A1* gene had been previously
470 implicated as the genetic variant underlying Steel syndrome[57–59]. Population screening
471 indicated that the disease variant is more common than previously thought in people
472 with Puerto Rican ancestry, and in some other Caribbean populations, and very rare or
473 absent elsewhere in the world. Extensive analysis of clinical records confirms almost all
474 features of the recessive disorder in cases, and reveals potential complications that can
475 occur later in life. An agnostic survey of the medical records of carriers, supplemented
476 by manual chart review, indicates evidence of joint and spine degradation in
477 heterozygotes. Biochemical modeling suggests that *COL27A1.*G697R disrupts a

bioRxiv preprint doi: https://doi.org/10.1101/141820; this version posted May 24, 2017. The copyright holder for this preprint (which was not certified by peer review) is the author/funder, who has granted bioRxiv a license to display the preprint in perpetuity. It is made available under aCC-BY-ND 4.0 International license.

478 conserved triple helix domain of the alpha-1 collagen in a mechanism similar to
479 dominant forms of other collagen disorders[63]. Taken together, this study indicates that a
480 single mutation in the *COL27A1* gene underlies a common collagen disorder impacting
481 up to 2% of people of Puerto Rican ancestry.

482 This is consistent with our finding, supported by previous work[50], demonstrating a
483 founder effect in Puerto Rican populations. Despite segregating at an estimated carrier
484 rate of 1:51, the *COL27A1.pG697R* variant was first described very recently[57]. This
485 suggests that there may be other highly penetrant disease variants segregating at
486 appreciable frequencies in Puerto Rican populations[89–94], and other understudied
487 founder populations, the discovery of which could lead to new disease variants and
488 biology. Indeed, although *COL27A1* was first implicated as the Steel syndrome disease
489 locus in an extended family from Puerto Rico recently[56], other variants in *COL27A1*
490 have since been linked to Steel syndrome in Indian[95] and Emerati[96] families revealing
491 additional clinical features of the disease such as hearing loss. In our own health
492 system, approximately 190,000 patients of Puerto Rican descent are treated annually[97].
493 We estimate that up to 80 may have the severe homozygous form of the disorder and
494 that the milder heterozygous form could be found in up to 1200 patients. A search of
495 progress notes, discharge summaries, and operative reports of over 4 million patients in
496 the Mount Sinai data warehouse discovered mentions of the text term “Steel Syndrome”
497 in 42 patient records. However, all of these patients were on dialysis for end stage renal
498 disease, indicating that this mention was a misspelling of vascular Steal Syndrome,
499 which is common in dialysis patients. This suggests that Steel syndrome might be
500 largely undiagnosed. Attempts are currently being made to re-contact Bio*Me*

bioRxiv preprint doi: https://doi.org/10.1101/141820; this version posted May 24, 2017. The copyright holder for this preprint (which was not certified by peer review) is the author/funder, who has granted bioRxiv a license to display the preprint in perpetuity. It is made available under aCC-BY-ND 4.0 International license.

501 participants with suspected Steel syndrome, and a genetic test is now available at
502 Mount Sinai (website: http://sema4genomics.com/products/test-catalog/).

503 This study highlights the benefits of incorporating statistical and population genetics
504 approaches in medical genetic research. First, we demonstrated that leveraging distant
505 relationships *via* IBD mapping was better powered for discovery of the *COL27A1* variant
506 compared to a more typical GWAS approach (i.e. genotype, imputation, and SNP
507 association). As sample sizes increase in health systems and biobanks, the odds of a
508 new individual being a direct or distant relative of someone already in the database
509 increases exponentially[98], enabling the detection of shared haplotypes harboring rarer
510 causal variants and better-powered IBD mapping studies. Second, we inferred that
511 *COL27A1*.pG697R variant arose on a Native American haplotype, and we estimate that
512 the allele may have segregated at a carrier frequency of 25-30% in pre-Columbian
513 Taíno populations and/or been driven to it's current frequency by a bottleneck that
514 occurred during the early days of colonization in Puerto Rico. Therefore this study not
515 only helps estimate population attributable risk of *COL27A1*.pG697R in Puerto Rican
516 populations, but also to predict other populations potentially at risk, including other
517 Caribbean and Taíno populations. Targeted population screening of *COL27A1*.pG697R
518 could potentially provide personalized health management, surveillance for associated
519 complications, guidelines for intervention (particularly in newborns[59]), and improved
520 reproductive choices.

521 This work also highlights some of the current challenges in the emerging field of
522 genomic medicine. We demonstrated that evidence from EHRs could be readily
523 extracted and retrospectively used to characterize clinical features of a musculoskeletal

bioRxiv preprint doi: https://doi.org/10.1101/141820; this version posted May 24, 2017. The copyright holder for this preprint (which was not certified by peer review) is the author/funder, who has granted bioRxiv a license to display the preprint in perpetuity. It is made available under aCC-BY-ND 4.0 International license.

524 genetic disorder. However, features of many other genetic disorders may not be
525 detectable via routine clinical exam, lab tests and radiologics, and may not be amenable
526 to such an approach. Furthermore, statistical methods for population-scale disease
527 variant discovery, which were predominantly developed for cohorts collected for genetic
528 research, may not be optimally calibrated for discovery in patient populations
529 encountered in health systems. Finally, many genetic disorders are very rare, or have
530 more complex genetic underpinnings, which would reduce power for detection using the
531 strategy we have described. However, recent efforts, such as the Precision Medicine
532 Initiative, that focus on the broad adoption of genomics in medicine, combined with
533 international efforts to catalog rare genetic diseases, are primed to increase the rate of
534 incidental genetic diagnosis of disease.

535 In summary, this work demonstrates the utility of biobanks for exploring full medical
536 phenomes, and highlights the importance of documenting a wider spectrum of genetic
537 disorders, in large and diverse populations of humans. In particular, this method
538 provides a bridge between classical medical genetic methods and those employed in
539 population-level GWAS. Here we note that the *COL27A1* variant is very rare in current
540 large-scale genomic databases used for clinical research. Thus traditional association
541 strategies and ascertainment bias focused on populations of European descent would
542 have failed to identify and characterize this disorder and its public health burden. As
543 ours and other recent studies have demonstrated, EHR-embedded research will be
544 increasingly important for disentangling the pathology of rare genetic disorders, and
545 understanding the continuum of complex and Mendelian disease. As studies grow in
546 size, and healthcare systems learn to leverage the wealth of information captured in the

bioRxiv preprint doi: https://doi.org/10.1101/141820; this version posted May 24, 2017. The copyright holder for this preprint (which was not certified by peer review) is the author/funder, who has granted bioRxiv a license to display the preprint in perpetuity. It is made available under aCC-BY-ND 4.0 International license.

547 EHR, there is a need to provide relevant medical information to any patient entering the
548 clinic anywhere in the world. Methods like that described here allow for precision
549 medicine with a truly global outlook.

550 **Materials and Methods**

551 *BioMe Biobank Program*

552 Study participants were recruited from the Bio*Me* Biobank Program of The Charles
553 Bronfman Institute for Personalized Medicine at Mount Sinai Medical Center from 2007
554 onward. The Bio*Me* Biobank Program (Institutional Review Board 07–0529) operates
555 under a Mount Sinai Institutional Review Board-approved research protocol. All study
556 participants provided written informed consent. Of the approximately 38000 participants
557 currently enrolled in Bio*Me,* N=10511 unrelated are genotyped on the Illumina Infinium
558 OmniExpress (OMNI) array. 5102 of these participants self-report as “Hispanic or
559 Latino”, 3080 as “African American or African”, 2078 as “White or Caucasian”, 89 as
560 “Mixed” and 162 as “Other”. Country of origin information is available for all but N=5
561 participants, with N=6553 reporting being born in the United States and the remaining
562 N=3953 report being born outside of the US. Parental and grandparental country of
563 origin information is only available for a small subset of individuals genotyped on the
564 OMNI array (N=43). An additional N=10471 participants were genotyped on the Illumina
565 Infinium Multi Ethnic Genotyping array (MEGA) v1.0. Of these, approximately 4704 self-
566 reported “Hispanic or Latino” ethnicity, 3143 self-reported as “African American or
567 African”, 22 self-reported as “White/Caucasian”, 708 self-reported as “Mixed” and 1894
568 self-reported as “Other”. Country of birth information was available for all but a small

bioRxiv preprint doi: https://doi.org/10.1101/141820; this version posted May 24, 2017. The copyright holder for this preprint (which was not certified by peer review) is the author/funder, who has granted bioRxiv a license to display the preprint in perpetuity. It is made available under aCC-BY-ND 4.0 International license.

569 number of participants (N=228), with 5190 reporting being born in the United States,
570 and the remaining 5053 self-reporting being born elsewhere. Parental and
571 grandparental country of origin information is available for 4323 individuals genotyped
572 on the MEGA array.

573 *OmniExpress Genotyping and QC*

574 Genotyping of 12749 Bio*Me* participants was performed on the Illumina Infinium
575 OmniExpress plus HumanExome array. Calling was performed using the
576 GenomeStudio software. A total of 1093 individuals were removed prior to zCall due to
577 plate failure (N=672), unambiguous discordance between genetic and EHR recorded
578 sex (N=693), a call rate of <98% (N=834), or deviances in levels of heterozygosity
579 (N=773 in total). This was defined as having either an inbreeding coefficient outside the
580 range -0.1 and 0.3 for common alleles (MAF >1%), or between 0.4 and 0.9 for rare
581 alleles (MAF <1%). Additional quality control of 11656 individuals was performed using
582 PLINK1.7[55] (RRID:SCR_001757). An individual with a call rate of <99% was also
583 excluded (N=1), along with intentional genetic duplicates (PiHat >0.8, N=444). Site-level
584 quality control consisted of the removal of SNPs with a call rate of <95% (n=42217), and
585 the removal of sites that were significantly out of Hardy-Weinberg equilibrium ($p<1x10^{-5}$;
586 n=39660) when calculated for self-reported EA, AA and H/L separately. Palindromic
587 sites and those that deviated considerably from the 1000 Genomes project allele
588 frequencies (<40% *versus* >60%) were also removed to ensure uniform stranding
589 across datasets. After QC steps, 11212 participants and 866864 SNPs remained for
590 downstream analysis.

bioRxiv preprint doi: https://doi.org/10.1101/141820; this version posted May 24, 2017. The copyright holder for this preprint (which was not certified by peer review) is the author/funder, who has granted bioRxiv a license to display the preprint in perpetuity. It is made available under aCC-BY-ND 4.0 International license.

591 *IBS Relatedness Estimates and Estimation of Inbreeding Co-efficient*

592 Pairwise IBS-based relationship estimates were derived for Bio*Me* participants
593 (N=11212) using the RELATEAdmix software[41], which accounts for inflation of IBS
594 statistic due to admixture linkage disequillibrium in admixed populations**.** To include
595 allele frequency information and global ancestry proportions from ancestral populations
596 relevant for each admixed population in the analysis. These were estimated using
597 ADMIXTURE[99] (RRID:SCR_001263) H/L samples were merged with the Utah
598 Residents (CEPH) with Northern and Western European Ancestry (CEU; N=100),
599 Yoruba in Ibadan, Nigeria (YRI; N=100) and Native American (NA; N=43; including
600 Nauha, Ayamaran, Mayan and Quechan individuals) and used as input for the
601 ADMIXTURE software, which was run unsupervised at k=3. ADMIXTURE analysis
602 confirmed that NA reference panel comprised > 99% proportion Native American
603 genetic ancestry (**Figure 4 – figure supplement 2**). European-American (EA)
604 individuals were merged with the CEU and a panel of self-reported Ashkenazi Jewish
605 individuals genotyped on OMNI from Bio*Me* (AJ; N=100) and run unsupervised at k=2.
606 AA samples were merged with the CEU and YRI reference panels and run
607 unsupervised at k=2. After intersecting with reference panels 99296 SNPs were used as
608 the input for RELATEAdmix..

609 *Principal Component Analysis*

610 Principal Component Analysis (PCA) was performed using the SMARTPCAv10210
611 software from the EIGENSOFTv5.0.1 (RRID:SCR_004965)[44] in 10511 unrelated Bio*Me*
612 participants. Regions containing the Human Leukocyte Antigen (chr6: 27000000-

bioRxiv preprint doi: https://doi.org/10.1101/141820; this version posted May 24, 2017. The copyright holder for this preprint (which was not certified by peer review) is the author/funder, who has granted bioRxiv a license to display the preprint in perpetuity. It is made available under aCC-BY-ND 4.0 International license.

613 35000000 (NCBI37/hg19)), Lactase gene (chr2:135000000-137000000 (NCBI37/hg19))
614 and a common inversion (chr8:6000000-16000000 (NCBI37/hg19)), all of which are
615 regions known to confound PCA analysis were removed from the genotype data prior to
616 analysis. Data were merged with a reference panel of 2504 individuals from Phase 3 of
617 the 1000 Genomes project (RRID:SCR_006828)[42] that was constructed by extracting
618 OmniExpress sites from whole-genome sequence data. Following this, a further two
619 other relevant reference panels were added: a the NA (N=43), and a AJ (N=100) panels
620 described above. A total of 174468 SNPs remained after intersecting the data with
621 these reference panels.

622 *Identity-by-Descent Tract Inference and Clustering*

623 Phased genotype data were filtered to MAF > 0.01 and converted to PLINK format using
624 the FCGENE software[100] (we avoided using PLINK software for the conversion process
625 in order to retain the phase information). Recombination maps from HapMap II (Build
626 GRCh37/hg19) were intersected with the genotyped sites (n=490510 SNPs).
627 GERMLINE (RRID:SCR_001720)[45] was used to infer tracts of identity by descent > 3cM
628 across all pairs of Bio*Me* individuals (N=11212) using the following flags*: "-min_m 3 -*
629 *err_hom 0 -err_het 2 -bits 25 –haploid".* IBD haplotypes that fell within or overlapped
630 with centromeres, telomeres and regions of low complexity were removed from the
631 GERMLINE output using an in-house Ruby script. Additional quality control measures
632 consisted of the exclusion of regions of the genome where the depth of IBD-sharing
633 (that is, the number of pairwise IBD-haplotypes that contain a given locus of the

bioRxiv preprint doi: https://doi.org/10.1101/141820; this version posted May 24, 2017. The copyright holder for this preprint (which was not certified by peer review) is the author/funder, who has granted bioRxiv a license to display the preprint in perpetuity. It is made available under aCC-BY-ND 4.0 International license.

634 genome) exceeded 4 standard deviations from the genome-wide mean (**Figure 2 –**
635 **figure supplement 6**).

636 IBD clustering to identify ‘cliques' of three or more IBD haplotypes shared between
637 multiple individuals was then performed using the efficient connect-component-based
638 clustering version of the Dash Associated Shared Haplotypes algorithm (DASH)[101]**,**
639 using the default parameters. As a further quality control measure IBD-sharing ‘cliques’
640 inferred by DASH that exhibited excessive sharing (which we defined as clique
641 membership that exceeded 4 s.d. above the genome-wide mean) were removed
642 (**Figure 2 –figure supplement 7**). Data was outputted from DASH in PLINK tped
643 format, and alleles were encoded as; homozygote member in a clique as “2”,
644 heterozygote member as “1” and everyone else not a member in the clique encoded as
645 “0”.

646 *Population-level IBD sharing*

647 We calculated the length of any pairwise IBD tract (or sum of the lengths if a pair of
648 individuals shared more than one tract IBD) for each IBD sharing pair within each
649 population to obtain an estimate of the mean and variance of pairwise sharing per
650 population. To compare the tract length distribution between populations (of size N), we
651 first binned pairwise IBD tracts by length bin in 0.01cM increments. We then summed
652 the number of pairwise IBD tracts falling into each length bin (x), and divided this
653 number by the number of possible pairwise IBD sharing for each population: N*(N-1)/2.

654 *Height Measurement and Transformation*

bioRxiv preprint doi: https://doi.org/10.1101/141820; this version posted May 24, 2017. The copyright holder for this preprint (which was not certified by peer review) is the author/funder, who has granted bioRxiv a license to display the preprint in perpetuity. It is made available under aCC-BY-ND 4.0 International license.

655 A self-reported measurement of height in feet and inches was recorded for each
656 participant at enrollment into the Bio*Me* program. Raw height data were stratified on the
657 basis of sex for all individuals who were inferred to be of Puerto Rican ancestry
658 (N=2816). Height data was then log transformed and converted to age-adjusted Z-
659 scores. Participants were excluded on the basis of age reported at the point of
660 enrollment, with a minimum cut-off of 18 years old for females (N=0) and 22 for males
661 (N=0), and a maximum cut off of 79 years old for both sexes (N=194) leaving a total of
662 n=2622 PR.

663 *Association of IBD-cliques with height under a recessive model*

664 Association of IBD clique membership with height as a continuous trait was performed
665 under a recessive model using PLINKv1.9[56] using the *"--linear recessive*" flag. Age and
666 sex adjusted Z-scores for height were used as the outcome variable. IBD clique
667 membership was used as the primary predictor variable and the first five PCA
668 eigenvectors were used as covariates. The model was run across a total of 2622 PR
669 ancestry individuals and a total of 480 IBD-cliques where at least 3 individuals were
670 homozygous for the IBD haplotype.

671 *Genome Wide Association of Imputed Data under a Recessive Model*

672 Genotype data for all of the Bio*Me* individuals ascertained on the Illumina OMNI
673 Express array (N=11212) were phased together using SHAPEIT2[102,103]. Imputation was
674 subsequently performed in 5MB chunks using IMPUTE2 (RRID:SCR_013055)[104] *via* the
675 flags *'-Ne 20000 -buffer 250 -filt_rules_l 'ALL<0.0002' 'ALL>0.9998''* with a reference

bioRxiv preprint doi: https://doi.org/10.1101/141820; this version posted May 24, 2017. The copyright holder for this preprint (which was not certified by peer review) is the author/funder, who has granted bioRxiv a license to display the preprint in perpetuity. It is made available under aCC-BY-ND 4.0 International license.

676 panel derived from Phase 3 data from the 1000 Genomes project. A total of 46538253
677 SNPs were imputed from 828109 directly genotyped SNPs.
678
679 We ran a recessive GWAS on the same 2622 inferred Puerto Rican ancestry individuals
680 used in our recessive IBD-mapping model. The association was run over hard-called
681 data using the PLINKv1.9 software using the *"--linear recessive*" flag. Age and sex
682 adjusted Z-scores for height were used as the phenotypic outcome and the first five PC
683 eigenvectors were used as covariates. Analysis was restricted to SNPs with >=2
684 observations of individuals homozygous for the minor allele (as the only 2 of the 3
685 homozygotes had been imputed correctly), and SNPs with an INFO score of >=0.3
686 (n=10007795 SNPs in total).

687 *Whole Genome Sequencing*

688 Genomic libraries were prepared from DNA obtained for the four IBD homozygous
689 individuals. DNA was sheared to 300 bp on a Covaris E220, libraries were made using
690 the NEBNext Ultra DNA Library Prep kit for Illumina. The libraries were submitted for
691 Whole Genome Sequencing (WGS) at the Mount Sinai Genomic Core using the Illumina
692 HiSeq 2500 system, performed by the Genomics Core Facility of the Icahn Institute for
693 Genomics and Multiscale Biology, Icahn School of Medicine at Mount Sinai. Reads
694 were aligned to the NCBI37/hg19 reference genome and variants were called using the
695 sequence analysis pipeline by Linderman *et al*[105] Variant calls and coverage at every
696 site at the genomic interval spanned by the candidate IBD haplotype (chr9:112000000-
697 118000000bp (NCBI37/hg19)) were obtained using the *"-out_mode EMIT_ALL_SITES*"

bioRxiv preprint doi: https://doi.org/10.1101/141820; this version posted May 24, 2017. The copyright holder for this preprint (which was not certified by peer review) is the author/funder, who has granted bioRxiv a license to display the preprint in perpetuity. It is made available under aCC-BY-ND 4.0 International license.

698 flag in GATKv3.2-72 (RRID:SCR_001876). For summary statistics of whole genome
699 sequencing (WGS) see **Supplement file 1**.

700 *In Silico analysis and validation of COL27A1.*pG967R

701 WGS variant calls were annotated with allele frequency information and *in silico*
702 prediction scores for SIFT, PhyloP, GERP generated using snpEffv3.0
703 (RRID:SCR_005191) as part of the sequence analysis pipeline published by Linderman
704 *et al*[105]. We identified all genomic variants that were present in at least 6 copies across
705 the four IBD-homozygotes and that lay within the shared boundary of the IBD haplotype.
706 Using this criteria, only one rare, coding variant was found to be shared between all four
707 homozygotes, namely a point mutation in the gene *COL27A1* (g.9:*116958257.C>G,*
708 NM_032888.1, p.G697R*,* rs140950220*)* which was present in 7 copies (with 3
709 individuals being homozygous, and the fourth being heterozygous). The rs140950220
710 G/C allele status was validated by Sanger sequencing of exon 7 in the *COL27A1* gene
711 in all four individuals. We also validated *COL27A1.*pG697R status in individuals carrying
712 the significant IBD-clique at 9q32 using the Fluidigm SNPType assay adhering to the
713 standard protocol. All individuals carrying at least one copy of the top IBD-haplotype
714 (N=59) were genotyped for the rs140950220 variant in addition to a panel of age and
715 sex matched Puerto Rican ancestry controls (N=59).

716 *Genotyping COL27A1.pG697R in a Multi-Ethnic Population of PAGE*

717 We estimated the frequency of the *COL27A1.pG697R (*dbSNP=rs140950220) variant in
718 the Population Architecture using Genomics and Epidemiology (PAGE) study. The

bioRxiv preprint doi: https://doi.org/10.1101/141820; this version posted May 24, 2017. The copyright holder for this preprint (which was not certified by peer review) is the author/funder, who has granted bioRxiv a license to display the preprint in perpetuity. It is made available under aCC-BY-ND 4.0 International license.

719 PAGE study comprises a diverse global reference panel from five studies. African-
720 American and Hispanic/Latino women from the Women's Health Initiative (WHI), a
721 multi-center cohort study investigating post-menopausal women's health in the US and
722 recruited women at 40 centers across the US. Self-identified Hispanic/Latinos from four
723 sites in San Diego, CA, Chicago, IL, Bronx, NY, and Miami, FL as part of the Hispanic
724 Community Health Study / Study of Latinos (HCHS/SOL). African American, Japanese
725 American, and Native Hawaiian participants from the Multiethnic Cohort (MEC)
726 prospective cohort study recruiting men and women from Hawaii and California. The
727 Global Reference Panel (GRP) created by Stanford University contributed samples
728 including; a population sample of Andean individuals primarily of Quechuan/Aymaran
729 ancestry from Puno, Peru; a population sample of Easter Island (Rapa Nui), Chile;
730 individuals of indigenous origin from Oaxaca, Mexico, Honduras, Colombia, the Nama
731 and Khomani KhoeSan populations of the Northern Cape, South Africa; the Human
732 Genome Diversity Panel in collaboration with the Centre Etude Polymorphism Humain
733 (CEPH) in Paris; and the Maasai in Kinyawa, Kenya (MKK) dataset from the
734 International Hapmap Project hosted at Coriell. Finally, the Bio*Me* biobank in the Mount
735 Sinai health system, New York City, contributed African-American, Hispanic/Latino, and
736 participants who reported as mixed or other ancestry to the PAGE study, ~50% of whom
737 were born outside New York City and for whom country-of-birth information was
738 available. In all, participants in the PAGE Study represent a global reference panel of
739 112 populations ranging from 4-17773 individuals in size (**Supplement file 4**). Samples
740 in the PAGE study were genotyped on the Illumina Multi-Ethnic Genotyping Array
741 (MEGA), which included direct genotyping of the rs140950220 variant. A total of 53338

bioRxiv preprint doi: https://doi.org/10.1101/141820; this version posted May 24, 2017. The copyright holder for this preprint (which was not certified by peer review) is the author/funder, who has granted bioRxiv a license to display the preprint in perpetuity. It is made available under aCC-BY-ND 4.0 International license.

742 PAGE and GRP samples were genotyped on the MEGA array at the Johns Hopkins
743 Center for Inherited Disease Research (CIDR), with 52878 samples successfully
744 passing CIDR's QC process. Genotyping data that passed initial quality control at CIDR
745 were released to the Quality Assurance / Quality Control (QA/QC) analysis team at the
746 University of Washington Genetics Coordinating Center (UWGCC). The UWGCC
747 further cleaned the data according to previously described methods[106] and returned
748 genotypes for 51520 subjects. A total of 1705969 SNPs were genotyped on the
749 MEGA. The *COL27A1*.pG697R variant passed the following filters; (1) CIDR technical
750 filters, (2) SNPs with missing call rate >= 2%, (3) SNPs with more than 6 discordant
751 calls in 988 study duplicates, (4) SNPs with greater than 1 Mendelian errors in 282 trios
752 and 1439 duos, (5) SNPs with a Hardy-Weinberg $p<10^{-10}$, (6) positional duplicates.

753 *Structural modeling of the COL27A1.PG697R missense variant*

754 We downloaded X-ray crystal coordinates (1CAG from Bella *et al*[64].; www.pdb.org) on
755 January 21, 2017. Visualization and modeling of the missense variant were performed
756 in PyMol (www.pymol.org; RRID:SCR_000305).
757

758 *Phenome-Wide Association Study*

759 To test for clinical symptoms of Steel syndrome in *COL27A1*.pG967R carriers, we
760 performed a Phenome-Wide Association Study (PheWas) with EHR-derived ICD9 billing
761 codes as the phenotypic outcome. In the association model, for each individual ICD9
762 codes were encoded as "1" if the ICD9 was present in their EHR, and "0" if the ICD9
763 code was absent. Carrier status for *COL27A1*.pG697R was used as the primary

bioRxiv preprint doi: https://doi.org/10.1101/141820; this version posted May 24, 2017. The copyright holder for this preprint (which was not certified by peer review) is the author/funder, who has granted bioRxiv a license to display the preprint in perpetuity. It is made available under aCC-BY-ND 4.0 International license.

764 predictor variable, with heterozygous individuals encoded as "1", non-carriers encoded
765 a "0" and homozygotes excluded from the analysis. We restricted the analysis to
766 carriers of *COL27A1*.pG697R (n=106) and non-carriers (n=4480) who either reported
767 being born in Puerto Rico or who were US-born, self-identified as H/L and overlapped
768 with Puerto Rican born individuals in principal component analysis. Age, sex and the
769 first 5 principal components were included as covariates in our model. The regression
770 was performed using four methods; Generalized Linear Models (GLM) using the glm()
771 function in Rv3.2.1; a score test based on the saddlepoint approximation (SPATest)
772 using the SPAtest() function in Rv3.2.1; a score test using a base adjustment for rare
773 variants (Firth test) using the logistf() function in Rv3.2.1; and a linear mixed model
774 using the GCTAv1.24.2 software with a genetic relationship matrix constructed from
775 281666 SNPs shared between the OMNI and MEGA arrays (MAF >= 1%). To adjust for
776 multiple tests, raw p-values were adjusted for false discovery rate using the p.adjust()
777 function in R, and only those below an FDR adjusted p-value of 0.05 were reported as
778 significant.

779 *Clinical review of patient records*

780 Information from inpatient, outpatient, emergency and private practice settings housed
781 in the Mount Sinai health system since 2004 was reviewed by two clinical experts
782 independently. This data includes laboratory reports, radiological data, pathology
783 results, operative and inpatient/outpatient progress notes, discharge summaries,
784 pharmacy, and nurses reports. The clinical experts examined for clinical features similar
785 to those reported for Steel syndrome cases in Flynn et al 2010[59], including

bioRxiv preprint doi: https://doi.org/10.1101/141820; this version posted May 24, 2017. The copyright holder for this preprint (which was not certified by peer review) is the author/funder, who has granted bioRxiv a license to display the preprint in perpetuity. It is made available under aCC-BY-ND 4.0 International license.

786 developmental dysplasia of the hip (or congenital hip dysplasia), carpal coalition,
787 scoliosis, and joint and spine anomalies. Both clinical experts reviews patient records
788 independently and compared notes to resolve discrepancies. They reviewed the records
789 of the 34 youngest *COL27A1*.pG697R carriers (mean age 42), and compared their
790 findings to 31 randomly selected age and sex matched Puerto Rican non-carriers, and
791 also to published reports of population prevalences of key clinical features for similar
792 age groups where available.

793 *Local Ancestry Estimation*

794 Due to the process of recombination, individuals from populations that have undergone
795 recent admixture can exhibit a mosaic of genetic ancestry along their genome. Their
796 genetic ancestry at a given genomic segment (referred to as local ancestry), can be
797 inferred from genotype data with the use of non-admixed reference panels of known
798 continental ancestry. We calculated local ancestry in the three homozygous Puerto
799 Rican individuals genotyped on OMNI by first extracting the intersecting sites of the
800 Affymetrix 6.0 array (n=593729 SNPs in total) and merging them with 3 ancestral
801 reference panels. These reference panels consisted of the CEU and YRI samples from
802 the 1000 Genomes Project in addition to the Native American reference panel described
803 previously that were used as a proxy for European, African and Native American
804 ancestral source populations, respectively. RFMix[84] was used to infer local ancestry.

805 *Calculation of Historical Effective Population Size in Puerto Ricans*

bioRxiv preprint doi: https://doi.org/10.1101/141820; this version posted May 24, 2017. The copyright holder for this preprint (which was not certified by peer review) is the author/funder, who has granted bioRxiv a license to display the preprint in perpetuity. It is made available under aCC-BY-ND 4.0 International license.

806 To investigate evidence of a founder effect in Puerto Ricans we ran the IBDNe
807 software[85] in 2816 Puerto Ricans from the discovery effort using the cleaned set of
808 pairwise IBD-haplotypes inferred using GERMLINE. IBDNe was run using the default
809 parameters, including an assumed generation time of 25 years.

810 **Acknowledgements**

811 We would like to thank Noah Zaitlen, Alexander Gusev, George Diaz, Rounak Dey, and
812 Alicia Martin for their helpful suggestions in preparing this manuscript. This work was
813 supported by funds from several grants; The Population Architecture Using Genomics
814 and Epidemiology (PAGE) program is funded by the National Human Genome
815 Research Institute, with co-funding from the National Institute on Minority Health and
816 Health Disparities, supported by U01HG007416, U01HG007417, U01HG007397,
817 U01HG007376, and U01HG007419. The PAGE consortium thanks the staff and
818 participants of all PAGE studies for their important contributions. The complete list of
819 PAGE members can be found at http://www.pagestudy.org. Genotyping services were
820 provided by the Center for Inherited Disease Research (CIDR). CIDR is fully funded
821 through a federal contract from the National Institutes of Health to The Johns Hopkins
822 University, contract number HHSN268201200008I. Genotype data quality control and
823 quality assurance services were provided by the Genetic Analysis Center in the
824 Biostatistics Department of the University of Washington, through support provided by
825 the CIDR contract. High performance computing was supported in part through the
826 computational resources and staff expertise provided by Scientific Computing at the
827 Icahn School of Medicine at Mount Sinai and through the Office of Research

bioRxiv preprint doi: https://doi.org/10.1101/141820; this version posted May 24, 2017. The copyright holder for this preprint (which was not certified by peer review) is the author/funder, who has granted bioRxiv a license to display the preprint in perpetuity. It is made available under aCC-BY-ND 4.0 International license.

828 Infrastructure under award number S10OD018522. The content is solely the
829 responsibility of the authors and does not necessarily represent the official views of the
830 National Institutes of Health.

831 **References**

832 1. Hamosh, A., Scott, A.F., Amberger, J., Valle, D., and McKusick, V.A. (2000). Online
833 Mendelian Inheritance in Man (OMIM). Hum. Mutat. *15*, 57–61.

834 2. McCarthy, J.J., McLeod, H.L., and Ginsburg, G.S. (2013). Genomic medicine: a
835 decade of successes, challenges, and opportunities. Sci. Transl. Med. *5*, 189sr4.

836 3. Bamshad, M.J., Ng, S.B., Bigham, A.W., Tabor, H.K., Emond, M.J., Nickerson, D. a.,
837 and Shendure, J. (2011). Exome sequencing as a tool for Mendelian disease gene
838 discovery - Supplementary information. Nat. Rev. Genet. *12*, 745–755.

839 4. Manolio, T. a, Chisholm, R.L., Ozenberger, B., Roden, D.M., Williams, M.S., Wilson,
840 R., Bick, D., Bottinger, E.P., Brilliant, M.H., Eng, C., et al. (2013). Implementing genomic
841 medicine in the clinic: the future is here. Genet. Med. *15*, 258–267.

842 5. Manolio, T.A., Abramowicz, M., Al-Mulla, F., Anderson, W., Balling, R., Berger, A.C.,
843 Bleyl, S., Chakravarti, A., Chisholm, R.L., Dissanayake, V.H.W., et al. (2015). Global
844 implementation of genomic medicine : We are not alone. Sci. Transl. Med. *7*, 1–8.

845 6. Philippakis, A.A., Azzariti, D.R., Beltran, S., Brookes, A.J., Brownstein, C.A., Brudno,
846 M., Brunner, H.G., Buske, O.J., Carey, K., Doll, C., et al. (2015). The Matchmaker
847 Exchange: A Platform for Rare Disease Gene Discovery. Hum. Mutat. *36*, 915–921.

848 7. Chong, J., Yu, J.-H., Lorentzen, P., Park, K., Jamal, S.M., Tabor, H.K., Rauch, A.,
849 Saenz, M.S., Boltshauser, E., Patterson, K.E., et al. (2015). Gene discovery for
850 Mendelian conditions via social networking: de novo variants in KDM1A cause
851 developmental delay and distinctive facial features. bioRxiv 028241.

852 8. Collins, F.S., and Varmus, H. (2015). A New Initiative on Precision Medicine. N. Engl.
853 J. Med. *372*, 793–795.

854 9. Ashley, E.A. (2015). The Precision Medicine Initiative. JAMA *313*, 2119.

855 10. Collins, R. (2012). What makes UK Biobank special? Lancet *379*, 1173–1174.

856 11. Dewey, F.E., Murray, M.F., Overton, J.D., Habegger, L., Leader, J.B., Fetterolf,
857 S.N., O'Dushlaine, C., Van Hout, C. V, Staples, J., Gonzaga-Jauregui, C., et al. (2016).

bioRxiv preprint doi: https://doi.org/10.1101/141820; this version posted May 24, 2017. The copyright holder for this preprint (which was not certified by peer review) is the author/funder, who has granted bioRxiv a license to display the preprint in perpetuity. It is made available under aCC-BY-ND 4.0 International license.

858 Distribution and clinical impact of functional variants in 50,726 whole-exome sequences
859 from the DiscovEHR study. Science *354*, aaf6814.

860 12. Feldman, G.L. (2016). 2016 ACMG Annual Meeting presidential address: the
861 practice of medical genetics: myths and realities. Genet. Med. *18*, 957–959.

862 13. Ashley, E.A. (2016). Towards precision medicine. Nat. Rev. Genet. *17*, 507–522.

863 14. Abul-Husn, N.S., Manickam, K., Jones, L.K., Wright, E.A., Hartzel, D.N., Gonzaga-
864 Jauregui, C., O'Dushlaine, C., Leader, J.B., Lester Kirchner, H., Lindbuchler, D.M., et al.
865 (2016). Genetic identification of familial hypercholesterolemia within a single U.S. health
866 care system. Science *354*, aaf7000.

867 15. Yang, Y., Muzny, D.M., Xia, F., Niu, Z., Person, R., Ding, Y., Ward, P., Braxton, A.,
868 Wang, M., Buhay, C., et al. (2014). Molecular Findings Among Patients Referred for
869 Clinical Whole-Exome Sequencing. JAMA *312*, 1870.

870 16. Taylor, J.C., Martin, H.C., Lise, S., Broxholme, J., Cazier, J.B., Rimmer, A.,
871 Kanapin, A., Lunter, G., Fiddy, S., Allan, C., et al. (2015). Factors influencing success of
872 clinical genome sequencing across a broad spectrum of disorders. Nat Genet *47*, 717–
873 726.

874 17. Chong, J.X., Buckingham, K.J., Jhangiani, S.N., Boehm, C., Sobreira, N., Smith,
875 J.D., Harrell, T.M., McMillin, M.J., Wiszniewski, W., Gambin, T., et al. (2015). The
876 Genetic Basis of Mendelian Phenotypes: Discoveries, Challenges, and Opportunities.
877 Am. J. Hum. Genet. *97*, 199–215.

878 18. Amendola, L.M., Jarvik, G.P., Leo, M.C., McLaughlin, H.M., Akkari, Y., Amaral,
879 M.D., Berg, J.S., Biswas, S., Bowling, K.M., Conlin, L.K., et al. (2016). Performance of
880 ACMG-AMP Variant-Interpretation Guidelines among Nine Laboratories in the Clinical
881 Sequencing Exploratory Research Consortium. Am. J. Hum. Genet. *99*, 247.

882 19. Katsanis, N. (2016). The continuum of causality in human genetic disorders.
883 Genome Biol. *17*, 233.

884 20. Manrai, A.K., Funke, B.H., Rehm, H.L., Olesen, M.S., Maron, B.A., Szolovits, P.,
885 Margulies, D.M., Loscalzo, J., and Kohane, I.S. (2016). Genetic Misdiagnoses and the
886 Potential for Health Disparities. N. Engl. J. Med. *375*, 655–665.

887 21. Popejoy, A.B., and Fullerton, S.M. (2016). Genomics is failing on diversity. Nature
888 *538*, 161–164.

889 22. Petrovski, S., Goldstein, D.B., Need, A., Goldstein, D., Bustamante, C., Burchard,
890 E., Vega, F., Price, A., Patterson, N., Plenge, R., et al. (2016). Unequal representation
891 of genetic variation across ancestry groups creates healthcare inequality in the
892 application of precision medicine. Genome Biol. *17*, 157.

bioRxiv preprint doi: https://doi.org/10.1101/141820; this version posted May 24, 2017. The copyright holder for this preprint (which was not certified by peer review) is the author/funder, who has granted bioRxiv a license to display the preprint in perpetuity. It is made available under aCC-BY-ND 4.0 International license.

893 23. Gottesman, O., Kuivaniemi, H., Tromp, G., Faucett, W.A., Li, R., Manolio, T. a,
894 Sanderson, S.C., Kannry, J., Zinberg, R., Basford, M. a, et al. (2013). The Electronic
895 Medical Records and Genomics (eMERGE) Network: past, present, and future. Genet.
896 Med. *15*, 761–771.

897 24. Green, R.C., Goddard, K.A.B., Jarvik, G.P., Amendola, L.M., Appelbaum, P.S.,
898 Berg, J.S., Bernhardt, B.A., Biesecker, L.G., Biswas, S., Blout, C.L., et al. (2016).
899 Clinical Sequencing Exploratory Research Consortium: Accelerating Evidence-Based
900 Practice of Genomic Medicine. Am. J. Hum. Genet. *98*, 1051–1066.

901 25. Blair, D.R., Lyttle, C.S., Mortensen, J.M., Bearden, C.F., Jensen, A.B., Khiabanian,
902 H., Melamed, R., Rabadan, R., Bernstam, E.V., Brunak, S., et al. (2013). A
903 Nondegenerate Code of Deleterious Variants in Mendelian Loci Contributes to Complex
904 Disease Risk. Cell *155*, 70–80.

905 26. Rehm, H.L., Berg, J.S., Brooks, L.D., Bustamante, C.D., Evans, J.P., Landrum,
906 M.J., Ledbetter, D.H., Maglott, D.R., Martin, C.L., Nussbaum, R.L., et al. (2015).
907 ClinGen--the Clinical Genome Resource. N. Engl. J. Med. *372*, 2235–2242.

908 27. Kirkpatrick, B.E., Riggs, E.R., Azzariti, D.R., Miller, V.R., Ledbetter, D.H., Miller,
909 D.T., Rehm, H., Martin, C.L., and Faucett, W.A. (2015). GenomeConnect: Matchmaking
910 Between Patients, Clinical Laboratories, and Researchers to Improve Genomic
911 Knowledge. Hum. Mutat. *36*, 974–978.

912 28. Gahl, W.A., Mulvihill, J.J., Toro, C., Markello, T.C., Wise, A.L., Ramoni, R.B.,
913 Adams, D.R., and Tifft, C.J. (2016). The NIH Undiagnosed Diseases Program and
914 Network: Applications to modern medicine. Mol. Genet. Metab. *117*, 393–400.

915 29. Browning, S.R., and Browning, B.L. (2011). Identity by Descent Between Distant
916 Relatives: Detection and Applications. Annu. Rev. Genet. *46*, 120920150949000.

917 30. Houwen, R.H., Baharloo, S., Blankenship, K., Raeymaekers, P., Juyn, J., Sandkuijl,
918 L.A., and Freimer, N.B. (1994). Genome screening by searching for shared segments:
919 mapping a gene for benign recurrent intrahepatic cholestasis. Nat. Genet. *8*, 380–386.

920 31. Kenny, E.E., Gusev, A., Riegel, K., Lütjohann, D., Lowe, J.K., Salit, J., Maller, J.B.,
921 Stoffel, M., Daly, M.J., Altshuler, D.M., et al. (2009). Systematic haplotype analysis
922 resolves a complex plasma plant sterol locus on the Micronesian Island of Kosrae. Proc.
923 Natl. Acad. Sci. U. S. A. *106*, 13886–13891.

924 32. Henden, L., Freytag, S., Afawi, Z., Baldassari, S., Berkovic, S.F., Bisulli, F.,
925 Canafoglia, L., Casari, G., Crompton, D.E., Depienne, C., et al. (2016). Identity by
926 descent fine mapping of familial adult myoclonus epilepsy (FAME) to 2p11.2???2q11.2.
927 Hum. Genet. 1–9.

bioRxiv preprint doi: https://doi.org/10.1101/141820; this version posted May 24, 2017. The copyright holder for this preprint (which was not certified by peer review) is the author/funder, who has granted bioRxiv a license to display the preprint in perpetuity. It is made available under aCC-BY-ND 4.0 International license.

928 33. Qi, L., Cornelis, M.C., Kraft, P., Stanya, K.J., Kao, W.H.L., Pankow, J.S., Dupuis, J.,
929 Florez, J.C., Fox, C.S., Paré, G., et al. (2010). Genetic variants at 2q24 are associated
930 with susceptibility to type 2 diabetes. Hum. Mol. Genet. *19*, 2706–2715.

931 34. Traherne, J.A., Jiang, W., Valdes, A.M., Hollenbach, J.A., Jayaraman, J., Lane, J.A.,
932 Johnson, C., Trowsdale, J., and Noble, J.A. (2016). KIR haplotypes are associated with
933 late-onset type 1 diabetes in European-American families. Genes Immun. *17*, 8–12.

934 35. Shaw, M., Yap, T.Y., Henden, L., Bahlo, M., Gardner, A., Kalscheuer, V.M., Haan,
935 E., Christie, L., Hackett, A., and Gecz, J. (2015). Identical by descent L1CAM mutation
936 in two apparently unrelated families with intellectual disability without L1 syndrome. Eur.
937 J. Med. Genet. *58*, 364–368.

938 36. Ko, J.M., Zhang, P., Law, S., Fan, Y., Song, Y.Q., Zhao, X.K., Wong, E.H.W., Tang,
939 S., Song, X., Lung, M.L., et al. (2014). Identity-by-descent approaches identify regions
940 of importance for genetic susceptibility to hereditary esophageal squamous cell
941 carcinoma. Oncol. Rep. *32*, 860–870.

942 37. Lalli, M.A., Cox, H.C., Arcila, M.L., Cadavid, L., Moreno, S., Garcia, G., Madrigal, L.,
943 Reiman, E.M., Arcos-Burgos, M., Bedoya, G., et al. (2014). Origin of the PSEN1 E280A
944 mutation causing early-onset Alzheimer's disease. Alzheimer's Dement. *10*, S277–
945 S283.

946 38. Visscher, P.M., McEvoy, B., and Yang, J. (2010). From Galton to GWAS:
947 quantitative genetics of human height. Genet. Res. (Camb). *92*, 371–379.

948 39. Lango Allen, H., Estrada, K., Lettre, G., Berndt, S.I., Weedon, M.N., Rivadeneira, F.,
949 Willer, C.J., Jackson, A.U., Vedantam, S., Raychaudhuri, S., et al. (2010). Hundreds of
950 variants clustered in genomic loci and biological pathways affect human height. Nature
951 *467*, 832–838.

952 40. Durand, C., and Rappold, G.A. (2013). Height matters-from monogenic disorders to
953 normal variation. Nat. Rev. Endocrinol. *9*, 171–177.

954 41. Moltke, I., and Albrechtsen, A. (2014). RelateAdmix: A software tool for estimating
955 relatedness between admixed individuals. Bioinformatics *30*, 1027–1028.

956 42. The 1000 Genomes Project Consortium (2015). A global reference for human
957 genetic variation. Nature *526*, 68–74.

958 43. Mao, X., Bigham, A.W., Mei, R., Gutierrez, G., Weiss, K.M., Brutsaert, T.D., Leon-
959 Velarde, F., Moore, L.G., Vargas, E., McKeigue, P.M., et al. (2007). A genomewide
960 admixture mapping panel for Hispanic/Latino populations. Am. J. Hum. Genet. *80*,
961 1171–1178.

bioRxiv preprint doi: https://doi.org/10.1101/141820; this version posted May 24, 2017. The copyright holder for this preprint (which was not certified by peer review) is the author/funder, who has granted bioRxiv a license to display the preprint in perpetuity. It is made available under aCC-BY-ND 4.0 International license.

44. Price, A.L., Patterson, N.J., Plenge, R.M., Weinblatt, M.E., Shadick, N.A., and Reich, D. (2006). Principal components analysis corrects for stratification in genome-wide association studies. Nat. Genet. *38*, 904–909.

45. Gusev, A., Lowe, J.K., Stoffel, M., Daly, M.J., Altshuler, D., Breslow, J.L., Friedman, J.M., and Pe'Er, I. (2009). Whole population, genome-wide mapping of hidden relatedness. Genome Res. *19*, 318–326.

46. Gusev, A., Palamara, P.F., Aponte, G., Zhuang, Z., Darvasi, A., Gregersen, P., and Pe'er, I. (2012). The architecture of long-range haplotypes shared within and across populations. Mol. Biol. Evol. *29*, 473–486.

47. Chiang, C.W.K., Ralph, P., and Novembre, J. (2016). Conflation of Short Identity-by-Descent Segments Bias Their Inferred Length Distribution. G3 (Bethesda). *6*, 1287–1296.

48. Browning, S.R., and Thompson, E.A. (2012). Detecting rare variant associations by identity-by-descent mapping in case-control studies. Genetics *190*, 1521–1531.

49. Need, A.C., Kasperaviciute, D., Cirulli, E.T., and Goldstein, D.B. (2009). A genome-wide genetic signature of Jewish ancestry perfectly separates individuals with and without full Jewish ancestry in a large random sample of European Americans. Genome Biol. *10*, R7.

50. Moreno-Estrada, A., Gravel, S., Zakharia, F., McCauley, J.L., Byrnes, J.K., Gignoux, C.R., Ortiz-Tello, P.A., Martínez, R.J., Hedges, D.J., Morris, R.W., et al. (2013). Reconstructing the Population Genetic History of the Caribbean. PLoS Genet. *9*,.

51. Durand, C., and Rappold, G. a (2013). Height matters-from monogenic disorders to normal variation. Nat. Rev. Endocrinol. *9*, 171–177.

52. eLife (2016). A century of trends in adult human height. Elife *5*, 1–29.

53. Cohen, P., Rogol, A.D., Deal, C.L., Saenger, P., Reiter, E.O., Ross, J.L., Chernausek, S.D., Savage, M.O., Wit, J.M., and 2007 ISS Consensus Workshop participants (2008). Consensus statement on the diagnosis and treatment of children with idiopathic short stature: a summary of the Growth Hormone Research Society, the Lawson Wilkins Pediatric Endocrine Society, and the European Society for Paediatric Endocrinology Workshop. J. Clin. Endocrinol. Metab. *93*, 4210–4217.

54. Vacic, V., Ozelius, L.J., Clark, L.N., Bar-Shira, A., Gana-Weisz, M., Gurevich, T., Gusev, A., Kedmi, M., Kenny, E.E., Liu, X., et al. (2014). Genome-wide mapping of IBD segments in an Ashkenazi PD cohort identifies associated haplotypes. Hum. Mol. Genet. *23*, 4693–4702.

bioRxiv preprint doi: https://doi.org/10.1101/141820; this version posted May 24, 2017. The copyright holder for this preprint (which was not certified by peer review) is the author/funder, who has granted bioRxiv a license to display the preprint in perpetuity. It is made available under aCC-BY-ND 4.0 International license.

996 55. Purcell, S., Neale, B., Todd-Brown, K., Thomas, L., Ferreira, M.A.R., Bender, D.,
997 Maller, J., Sklar, P., de Bakker, P.I.W., Daly, M.J., et al. (2007). PLINK: A tool set for
998 whole-genome association and population-based linkage analyses. Am. J. Hum. Genet.
999 *81*, 559–575.

1000 56. Chang, C.C., Chow, C.C., Tellier, L.C., Vattikuti, S., Purcell, S.M., and Lee, J.J.
1001 (2015). Second-generation PLINK: rising to the challenge of larger and richer datasets.
1002 Gigascience *4*, 7.

1003 57. Gonzaga-Jauregui, C., Gamble, C.N., Yuan, B., Penney, S., Jhangiani, S., Muzny,
1004 D.M., Gibbs, R.A., Lupski, J.R., and Hecht, J.T. (2015). Mutations in COL27A1 cause
1005 Steel syndrome and suggest a founder mutation effect in the Puerto Rican population.
1006 Eur. J. Hum. Genet. *23*, 342–346.

1007 58. Steel, H.H., Piston, R.W., Clancy, M., and Betz, R.R. (1993). A syndrome of
1008 dislocated hips and radial heads, carpal coalition, and short stature in Puerto Rican
1009 children. J. Bone Jt. Surg. - Ser. A.75 ()(pp 259-264), 1993.Date Publ. 1993. *75*, 259–
1010 264.

1011 59. Flynn, J.M., Ramirez, N., Betz, R., Mulcahey, M.J., Pino, F., Herrera-Soto, J. a,
1012 Carlo, S., and Cornier, A.S. (2010). Steel syndrome: dislocated hips and radial heads,
1013 carpal coalition, scoliosis, short stature, and characteristic facial features. J. Pediatr.
1014 Orthop. *30*, 282–288.

1015 60. Pace, J.M., Corrado, M., Missero, C., and Byers, P.H. (2003). Identification,
1016 characterization and expression analysis of a new fibrillar collagen gene, COL27A1.
1017 Matrix Biol. *22*, 3–14.

1018 61. Plumb, D.A., Ferrara, L., Torbica, T., Knowles, L., Mironov, A., Kadler, K.E., Briggs,
1019 M.D., and Boot-Handford, R.P. (2011). Collagen XXVII Organises the Pericellular Matrix
1020 in the Growth Plate. PLoS One *6*, e29422.

1021 62. Christiansen, H.E., Lang, M.R., Pace, J.M., and Parichy, D.M. (2009). Critical Early
1022 Roles for col27a1a and col27a1b in Zebrafish Notochord Morphogenesis, Vertebral
1023 Mineralization and Post-embryonic Axial Growth. PLoS One *4*, e8481.

1024 63. Persikov, A. V., Pillitteri, R.J., Amin, P., Schwarze, U., Byers, P.H., and Brodsky, B.
1025 (2004). Stability related bias in residues replacing glycines within the collagen triple
1026 helix (Gly-Xaa-Yaa) in inherited connective tissue disorders. Hum. Mutat. *24*, 330–337.

1027 64. Bella, J., Eaton, M., Brodsky, B., and Berman, H.M. (1994). Crystal and molecular
1028 structure of a collagen-like peptide at 1.9 A resolution. Science *266*, 75–81.

1029 65. McGrory, J., Costa, T., and Cole, W.G. (1996). A novel G499D substitution in the
1030 alpha 1(III) chain of type III collagen produces variable forms of Ehlers-Danlos
1031 syndrome type IV. Hum. Mutat. *7*, 59–60.

bioRxiv preprint doi: https://doi.org/10.1101/141820; this version posted May 24, 2017. The copyright holder for this preprint (which was not certified by peer review) is the author/funder, who has granted bioRxiv a license to display the preprint in perpetuity. It is made available under aCC-BY-ND 4.0 International license.

1032 66. Tromp, G., De Paepe, A., Nuytinck, L., Madhatheri, S., and Kuivaniemi, H. (1995).
1033 Substitution of valine for glycine 793 in type III procollagen in Ehlers-Danlos syndrome
1034 type IV. Hum. Mutat. *5*, 179–181.

1035 67. Anderson, D.W., Thakker-Varia, S., Tromp, G., Kuivaniemi, H., and Stolle, C.A.
1036 (1997). A glycine (415)-to-serine substitution results in impaired secretion and
1037 decreased thermal stability of type III procollagen in a patient with Ehlers-Danlos
1038 syndrome type IV. Hum. Mutat. *9*, 62–63.

1039 68. Knebelmann, B., Deschenes, G., Gros, F., Hors, M.C., Grünfeld, J.P., Zhou, J.,
1040 Tryggvason, K., Gubler, M.C., and Antignac, C. (1992). Substitution of arginine for
1041 glycine 325 in the collagen alpha 5 (IV) chain associated with X-linked Alport syndrome:
1042 characterization of the mutation by direct sequencing of PCR-amplified lymphoblast
1043 cDNA fragments. Am. J. Hum. Genet. *51*, 135–142.

1044 69. Zhou, J., Hertz, J.M., and Tryggvason, K. (1992). Mutation in the alpha 5(IV)
1045 collagen chain in juvenile-onset Alport syndrome without hearing loss or ocular lesions:
1046 detection by denaturing gradient gel electrophoresis of a PCR product. Am. J. Hum.
1047 Genet. *50*, 1291–1300.

1048 70. Starman, B.J., Eyre, D., Charbonneau, H., Harrylock, M., Weis, M.A., Weiss, L.,
1049 Graham, J.M., and Byers, P.H. (1989). Osteogenesis imperfecta. The position of
1050 substitution for glycine by cysteine in the triple helical domain of the pro alpha 1(I)
1051 chains of type I collagen determines the clinical phenotype. J. Clin. Invest. *84*, 1206–
1052 1214.

1053 71. Shapiro, J.R., Stover, M.L., Burn, V.E., McKinstry, M.B., Burshell, A.L., Chipman,
1054 S.D., and Rowe, D.W. (1992). An osteopenic nonfracture syndrome with features of
1055 mild osteogenesis imperfecta associated with the substitution of a cysteine for glycine at
1056 triple helix position 43 in the pro alpha 1(I) chain of type I collagen. J. Clin. Invest. *89*,
1057 567–573.

1058 72. Denny, J.C., Ritchie, M.D., Basford, M.A., Pulley, J.M., Bastarache, L., Brown-
1059 Gentry, K., Wang, D., Masys, D.R., Roden, D.M., and Crawford, D.C. (2010). PheWAS:
1060 Demonstrating the feasibility of a phenome-wide scan to discover gene-disease
1061 associations. Bioinformatics *26*, 1205–1210.

1062 73. Denny, J.C., Bastarache, L., Ritchie, M.D., Carroll, R.J., Zink, R., Mosley, J.D.,
1063 Field, J.R., Pulley, J.M., Ramirez, A.H., Bowton, E., et al. (2013). Systematic
1064 comparison of phenome-wide association study of electronic medical record data and
1065 genome-wide association study data. Nat. Biotechnol. *31*, 1102–1110.

1066 74. Dey, R., Schmidt, E.M., Abecasis, G.R., and Lee, S. (2017). A fast and accurate
1067 algorithm to test for binary phenotypes and its application to PheWAS. bioRxiv.

bioRxiv preprint doi: https://doi.org/10.1101/141820; this version posted May 24, 2017. The copyright holder for this preprint (which was not certified by peer review) is the author/funder, who has granted bioRxiv a license to display the preprint in perpetuity. It is made available under aCC-BY-ND 4.0 International license.

1068 75. Yang, J., Lee, S.H., Goddard, M.E., and Visscher, P.M. (2011). GCTA: a tool for
1069 genome-wide complex trait analysis. Am. J. Hum. Genet. *88*, 76–82.

1070 76. Wang, X. (2014). Firth logistic regression for rare variant association tests. Front.
1071 Genet. *5*, 187.

1072 77. Kebaish, K.M., Neubauer, P.R., Voros, G.D., Khoshnevisan, M.A., and Skolasky,
1073 R.L. (2011). Scoliosis in adults aged forty years and older: prevalence and relationship
1074 to age, race, and gender. Spine (Phila. Pa. 1976). *36*, 731–736.

1075 78. Reginster, J.Y. (2002). The prevalence and burden of arthritis. Rheumatology
1076 (Oxford). *41 Supp 1*, 3–6.

1077 79. Kolonel, L.N., Henderson, B.E., Hankin, J.H., Nomura, A.M., Wilkens, L.R., Pike,
1078 M.C., Stram, D.O., Monroe, K.R., Earle, M.E., and Nagamine, F.S. (2000). A multiethnic
1079 cohort in Hawaii and Los Angeles: baseline characteristics. Am. J. Epidemiol. *151*, 346–
1080 357.

1081 80. LaVange, L.M., Kalsbeek, W.D., Sorlie, P.D., Avilés-Santa, L.M., Kaplan, R.C.,
1082 Barnhart, J., Liu, K., Giachello, A., Lee, D.J., Ryan, J., et al. (2010). Sample Design and
1083 Cohort Selection in the Hispanic Community Health Study/Study of Latinos. Ann.
1084 Epidemiol. *20*, 642–649.

1085 81. (1998). Design of the Women's Health Initiative clinical trial and observational study.
1086 The Women's Health Initiative Study Group. Control. Clin. Trials *19*, 61–109.

1087 82. Cann, H.M., de Toma, C., Cazes, L., Legrand, M.-F., Morel, V., Piouffre, L., Bodmer,
1088 J., Bodmer, W.F., Bonne-Tamir, B., Cambon-Thomsen, A., et al. (2002). A human
1089 genome diversity cell line panel. Science *296*, 261–262.

1090 83. Lek, M., Karczewski, K.J., Samocha, K.E., Banks, E., Fennell, T., O, A.H., Ware,
1091 J.S., Hill, A.J., Cummings, B.B., Birnbaum, D.P., et al. (2016). Analysis of protein-coding
1092 genetic variation in 60,706 humans. bioRxiv *536*, 030338.

1093 84. Maples, B.K., Gravel, S., Kenny, E.E., and Bustamante, C.D. (2013). RFMix: A
1094 discriminative modeling approach for rapid and robust local-ancestry inference. Am. J.
1095 Hum. Genet. *93*, 278–288.

1096 85. Browning, S.R., and Browning, B.L. (2015). Accurate Non-parametric Estimation of
1097 Recent Effective Population Size from Segments of Identity by Descent. Am. J. Hum.
1098 Genet. *97*, 404–418.

1099 86. Gravel, S., Zakharia, F., Moreno-Estrada, A., Byrnes, J.K., Muzzio, M., Rodriguez-
1100 Flores, J.L., Kenny, E.E., Gignoux, C.R., Maples, B.K., Guiblet, W., et al. (2013).
1101 Reconstructing Native American migrations from whole-genome and whole-exome data.
1102 PLoS Genet. *9*, e1004023.

bioRxiv preprint doi: https://doi.org/10.1101/141820; this version posted May 24, 2017. The copyright holder for this preprint (which was not certified by peer review) is the author/funder, who has granted bioRxiv a license to display the preprint in perpetuity. It is made available under aCC-BY-ND 4.0 International license.

1103 87. Voight, B.F., Kudaravalli, S., Wen, X., and Pritchard, J.K. (2006). A map of recent
1104 positive selection in the human genome. PLoS Biol. *4*, e72.

1105 88. Szpiech, Z.A., and Hernandez, R.D. (2014). Selscan: An efficient multithreaded
1106 program to perform EHH-based scans for positive selection. Mol. Biol. Evol. *31*, 2824–
1107 2827.

1108 89. Anikster, Y., Huizing, M., White, J., Shevchenko, Y.O., Fitzpatrick, D.L., Touchman,
1109 J.W., Compton, J.G., Bale, S.J., Swank, R.T., Gahl, W. a, et al. (2001). Mutation of a
1110 new gene causes a unique form of Hermansky-Pudlak syndrome in a genetic isolate of
1111 central Puerto Rico. Nat. Genet. *28*, 376–380.

1112 90. Cornier, A.S., Staehling-Hampton, K., Delventhal, K.M., Saga, Y., Caubet, J.-F.,
1113 Sasaki, N., Ellard, S., Young, E., Ramirez, N., Carlo, S.E., et al. (2008). Mutations in the
1114 MESP2 Gene Cause Spondylothoracic Dysostosis/Jarcho-Levin Syndrome. Am. J.
1115 Hum. Genet. *82*, 1334–1341.

1116 91. Daniels, M.L.A., Leigh, M.W., Davis, S.D., Armstrong, M.C., Carson, J.L., Hazucha,
1117 M., Dell, S.D., Eriksson, M., Collins, F.S., Knowles, M.R., et al. (2013). Founder
1118 mutation in RSPH4A identified in patients of Hispanic descent with primary ciliary
1119 dyskinesia. Hum. Mutat. *34*, 1352–1356.

1120 92. Al-Zaidy, S.A., Malik, V., Kneile, K., Rosales, X.Q., Gomez, A.M., Lewis, S.,
1121 Hashimoto, S., Gastier-Foster, J., Kang, P., Darras, B., et al. (2015). A slowly
1122 progressive form of limb-girdle muscular dystrophy type 2C associated with founder
1123 mutation in the SGCG gene in Puerto Rican Hispanics. Mol. Genet. Genomic Med. *3*,
1124 92–98.

1125 93. Arnold, S.E., Vega, I.E., Karlawish, J.H., Wolk, D.A., Nunez, J., Negron, M., Xie,
1126 S.X., Wang, L.S., Dubroff, J.G., McCarty-Wood, E., et al. (2013). Frequency and
1127 clinicopathological characteristics of presenilin 1 Gly206Ala mutation in puerto rican
1128 hispanics with dementia. J. Alzheimer's Dis. *33*, 1089–1095.

1129 94. Lee, J.H., Kahn, A., Cheng, R., Reitz, C., Vardarajan, B., Lantigua, R., Medrano, M.,
1130 Jiménez-Velázquez, I.Z., Williamson, J., Nagy, P., et al. (2014). Disease-related
1131 mutations among Caribbean Hispanics with familial dementia. Mol. Genet. Genomic
1132 Med. *2*, 430–437.

1133 95. Kotabagi, S., Shah, H., Shukla, A., and Girisha, K.M. (2017). Second family
1134 provides further evidence for causation of Steel syndrome by biallelic mutations in
1135 *COL27A1*. Clin. Genet.

1136 96. Gariballa, N., Ben-Mahmoud, A., Komara, M., Al-Shamsi, A.M., John, A., Ali, B.R.,
1137 and Al-Gazali, L. (2017). A novel aberrant splice site mutation in *COL27A1* is
1138 responsible for Steel syndrome and extension of the phenotype to include hearing loss.
1139 Am. J. Med. Genet. Part A *173*, 1257–1263.

bioRxiv preprint doi: https://doi.org/10.1101/141820; this version posted May 24, 2017. The copyright holder for this preprint (which was not certified by peer review) is the author/funder, who has granted bioRxiv a license to display the preprint in perpetuity. It is made available under aCC-BY-ND 4.0 International license.

1140 97. Humes, K.R., Jones, N. a., and Ramirez, R.R. (2011). Overview of race and
1141 hispanic origin: 2010. Office 23.

1142 98. Henn, B.M., Hon, L., Macpherson, J.M., Eriksson, N., Saxonov, S., Pe'er, I., and
1143 Mountain, J.L. (2012). Cryptic distant relatives are common in both isolated and
1144 cosmopolitan genetic samples. PLoS One *7*,.

1145 99. Alexander, D.H., Novembre, J., and Lange, K. (2009). Fast model-based estimation
1146 of ancestry in unrelated individuals. Genome Res. *19*, 1655–1664.

1147 100. Roshyara, N.R., and Scholz, M. (2014). fcGENE: A Versatile Tool for Processing
1148 and Transforming SNP Datasets. PLoS One *9*, e97589.

1149 101. Gusev, A., Kenny, E.E., Lowe, J.K., Salit, J., Saxena, R., Kathiresan, S., Altshuler,
1150 D.M., Friedman, J.M., Breslow, J.L., and Pe'er, I. (2011). DASH: a method for identical-
1151 by-descent haplotype mapping uncovers association with recent variation. Am. J. Hum.
1152 Genet. *88*, 706–717.

1153 102. Delaneau, O., Marchini, J., and Zagury, J.-F. (2011). A linear complexity phasing
1154 method for thousands of genomes. Nat. Methods *9*, 179–181.

1155 103. O'Connell, J., Gurdasani, D., Delaneau, O., Pirastu, N., Ulivi, S., Cocca, M.,
1156 Traglia, M., Huang, J., Huffman, J.E., Rudan, I., et al. (2014). A general approach for
1157 haplotype phasing across the full spectrum of relatedness. PLoS Genet. *10*, e1004234.

1158 104. Howie, B.N., Donnelly, P., and Marchini, J. (2009). A flexible and accurate
1159 genotype imputation method for the next generation of genome-wide association
1160 studies. PLoS Genet. *5*, e1000529.

1161 105. Linderman, M.D., Brandt, T., Edelmann, L., Jabado, O., Kasai, Y., Kornreich, R.,
1162 Mahajan, M., Shah, H., Kasarskis, A., and Schadt, E.E. (2014). Analytical validation of
1163 whole exome and whole genome sequencing for clinical applications. BMC Med.
1164 Genomics *7*, 20.

1165 106. Laurie, C.C., Doheny, K.F., Mirel, D.B., Pugh, E.W., Bierut, L.J., Bhangale, T.,
1166 Boehm, F., Caporaso, N.E., Cornelis, M.C., Edenberg, H.J., et al. (2010). Quality control
1167 and quality assurance in genotypic data for genome-wide association studies. Genet.
1168 Epidemiol. *34*, 591–602.

1169

1170

bioRxiv preprint doi: https://doi.org/10.1101/141820; this version posted May 24, 2017. The copyright holder for this preprint (which was not certified by peer review) is the author/funder, who has granted bioRxiv a license to display the preprint in perpetuity. It is made available under aCC-BY-ND 4.0 International license.

1171 **Web Resources**

1172 *BioMe OmniExpress data:*

1173 https://www.ncbi.nlm.nih.gov/projects/gap/cgi-bin/study.cgi?study_id=phs000888.v1.p1

1174 *BioMe MEGA data:*

1175 https://www.ncbi.nlm.nih.gov/projects/gap/cgi-bin/study.cgi?study_id=phs000925

1176 *PAGE MEGA data:*

1177 https://www.ncbi.nlm.nih.gov/projects/gap/cgi-bin/study.cgi?study_id=phs000356

1178 *Location of Native American panels:*

1179 ftp://ftp.1000genomes.ebi.ac.uk/vol1/ftp/technical/working/20130711_native_ame

1180 rican_admix_train/

1181 *Software used in the analysis:*

1182 SMARTPCA: https://github.com/DReichLab/EIG

1183 ADMIXTURE: https://www.genetics.ucla.edu/software/admixture/download.html

1184 RelateAdmix: http://www.popgen.dk/software/index.php/RelateAdmix#Download

1185 RFMix: https://sites.google.com/site/rfmixlocalancestryinference/

1186 GERMLINE: http://www.cs.columbia.edu/~gusev/germline/

1187 DASH: http://www1.cs.columbia.edu/~gusev/dash/

1188 PyMol: www.pymol.org

1189 IBDNe: http://faculty.washington.edu/browning/ibdne.html

bioRxiv preprint doi: https://doi.org/10.1101/141820; this version posted May 24, 2017. The copyright holder for this preprint (which was not certified by peer review) is the author/funder, who has granted bioRxiv a license to display the preprint in perpetuity. It is made available under aCC-BY-ND 4.0 International license.

EHR-Documented Evidence	Literature Homozygous children	Literature Homozygous Adults	Bio*Me* Homozygous Adults	Bio*Me* Heterozygous Adults <55yoa	Bio*Me* Controls Adults <55yoa
N (N of females)	27 (9)	7(6)	5 (3)	34(20)	31(23)
Mean age (years)	12.8	35.4	51.6	41.8	40.6
EHR-Documented Medical History	**N(%)**	**N(%)**	**N(%)**	**N(%)**	**N(%)**
Height >= 2 s.d. from pop mean	27 (100)	7 (100)	5 (100)	0 (0)	0 (0)
Congenital hip dislocation			4	0	0
Leg length discrepancy			1	0	0
Total	27(100)	7(100)	5 (100)	0 (0)	0 (0)
Elbow contractures	24 (89)	7 (100)	1 (20)	0 (0)	0 (0)
Wrist deformity			1	2	1
Lunotriquetial fusion			1	0	0
Carpel tunnel			0	3	3
Total	24 (89)	6 (86)	2 (40)	5(15)	4(13)
Scoliosis	12 (44)	6 (86)	2 (40)	8 (24)	4 (13)
Pes cavus	12 (44)	0 (0)	0 (0)	0 (0)	0 (0)
Cervical stenosis			3	5	0
Cervical discitis			1	0	0
Cervical spondylosis			2	7	3
Cervical cord compression			3	3	1
Total	3 (9)	0 (0)	4 (80)	7 (21)	3 (10)
EHR-Documented Medical History			N(%)	N(%)	N(%)
Lumbar spine	-	-	1 (20)	10 (29)	5 (16)
Thoracic spine	-	-	1 (20)	5(15)	4(13)
Osteoporosis or osteopenia	-	-	3 (60)	3(9)	1 (3)
Arthritis or degenerative changes	-	-	3 (60)	13(38)	6 (19)
Hip replacement	-	-	3 (60)	0 (0)	0 (0)
Knee replacement	-	-	2 (40)	0 (0)	0 (0)
Cervical spine	-	-	3 (60)	2 (6)	1 (3)
Lumbar spine	-	-	1 (20)	1 (3)	0 (0)
Thoracic spine	-	-	2 (40)	1 (3)	1 (3)

Table 1 Clinical characteristics of five BioMe participants homozygote, thirty-four carriers and thirty-one non-carriers of the *COL27A1*.pG697R variant using evidence documented in Electronic Health Records (including billing and procedural codes, laboratory, radiologic, and progress notes) compared to features previously reported in Flynn et al, 2010, and Steel et al, 1993 for 27 children and 7 adults with Steel syndrome.

bioRxiv preprint doi: https://doi.org/10.1101/141820; this version posted May 24, 2017. The copyright holder for this preprint (which was not certified by peer review) is the author/funder, who has granted bioRxiv a license to display the preprint in perpetuity. It is made available under aCC-BY-ND 4.0 International license.

1199

Disease Category	ICD9 Code	Short description	Number of diagnoses among carriers N (%)	Number of diagnoses among non-carriers N (%)	Odds Ratio (5% confidence intervals)	P-value
Neoplasms	622.10	Dysplasia of cervix, not otherwise specified	6 (5.7)	62 (1.4)	5.4 (2.3-12.6)	1.0 x 10-4
Musculoskeletal	716.98	Arthropathy unspecified, involving other unspecified sites	4 (3.8)	48 (1.1)	5.8 (2.2-15.3)	4.4 x 10-4
Musculoskeletal	721.00	Cervical spondylosis without myelopathy	5 (4.5)	74 (1.6)	5.4 (2.4-12.3)	6.6 x 10-5
Musculoskeletal	730.08	Acute osteomyelitis involving other specified sites	3 (2.8)	6 (0.1)	34.5 (7.4-162)	7.1 x 10-6
Digestive	789.10	Hepatomegaly	3 (2.8)	17 (0.4	11.6 (3.2-42.2)	2.1 x 10-4

1200

1201 **Table 2** Top five significantly PheWAS associated ICD9 codes in *COL27A1*.pG697R
1202 carriers (N=106) compared to non-carriers (N=4480)

1203

1204

bioRxiv preprint doi: https://doi.org/10.1101/141820; this version posted May 24, 2017. The copyright holder for this preprint (which was not certified by peer review) is the author/funder, who has granted bioRxiv a license to display the preprint in perpetuity. It is made available under aCC-BY-ND 4.0 International license.

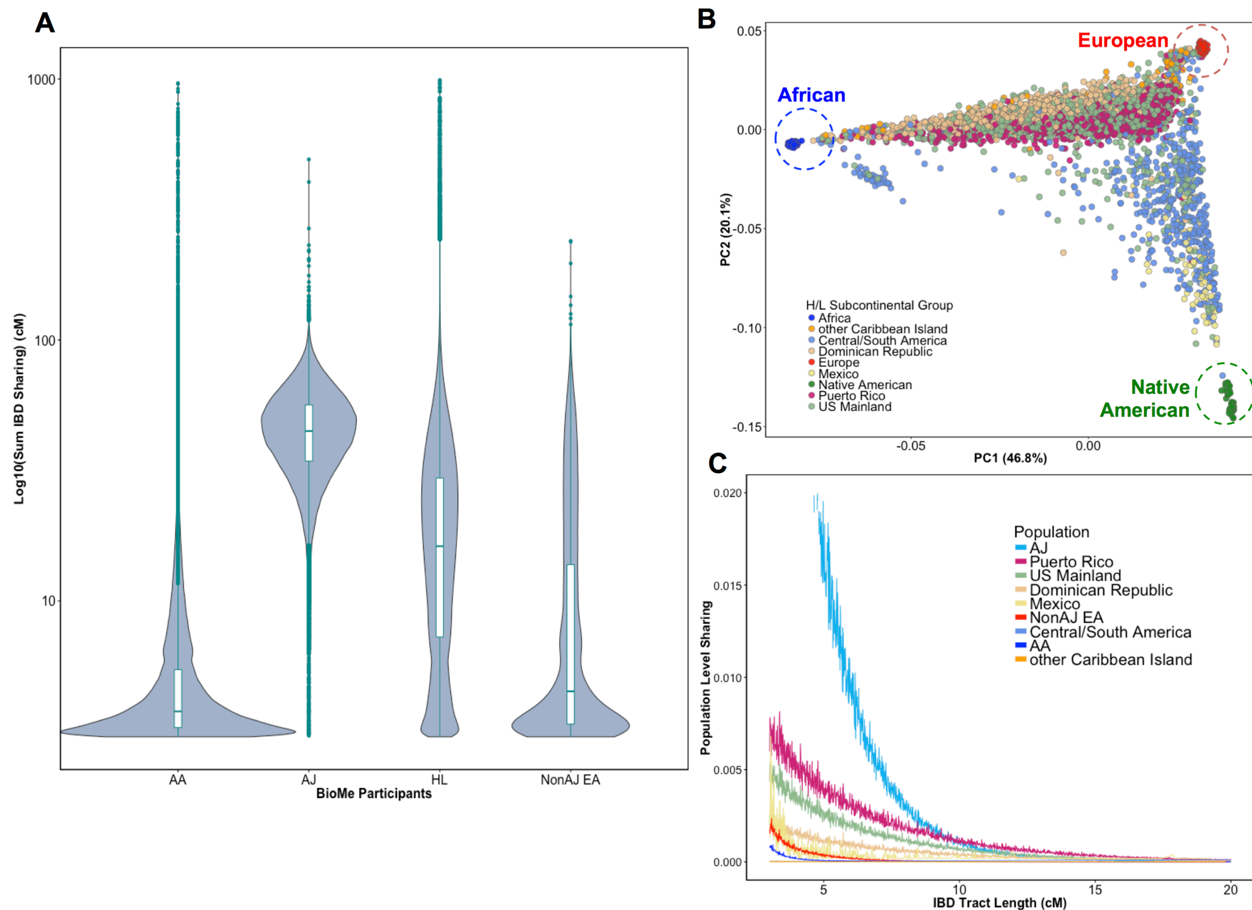

1205
1206 **Figure 1** (A) Distribution of the pairwise sum of Identity-by-Descent (IBD) sharing (cM)
1207 between four broadly defined Bio*Me* populations, namely; African American (AA),
1208 Ashkenazi Jewish (AJ), Hispanic/Latino (H/L) and Non-Jewish European American
1209 (Non-AJ EA). (B) Sub-continental diversity in self-reported H/L participants in Bio*Me.*
1210 Afro-Caribbean participants fall between European (red) and African (blue) continental
1211 reference panels, Mexican and Central/South American H/L participants fall between
1212 European and Native American (green) reference panels, mainland US-born
1213 participants reside on either cline. (C) The tract length distribution of IBD sharing among
1214 Bio*Me* populations, normalized by population size. The y-axis represents the proportion
1215 population-level sharing ($x / (N*(N-1)/2)$), where x is the sum of the number of pairwise

bioRxiv preprint doi: https://doi.org/10.1101/141820; this version posted May 24, 2017. The copyright holder for this preprint (which was not certified by peer review) is the author/funder, who has granted bioRxiv a license to display the preprint in perpetuity. It is made available under aCC-BY-ND 4.0 International license.

1216 shared IBD tracts and N is the number of individuals per population. The AJ population
1217 exhibits the highest level of population level sharing, followed by Puerto Rican born H/L.
1218

bioRxiv preprint doi: https://doi.org/10.1101/141820; this version posted May 24, 2017. The copyright holder for this preprint (which was not certified by peer review) is the author/funder, who has granted bioRxiv a license to display the preprint in perpetuity. It is made available under aCC-BY-ND 4.0 International license.

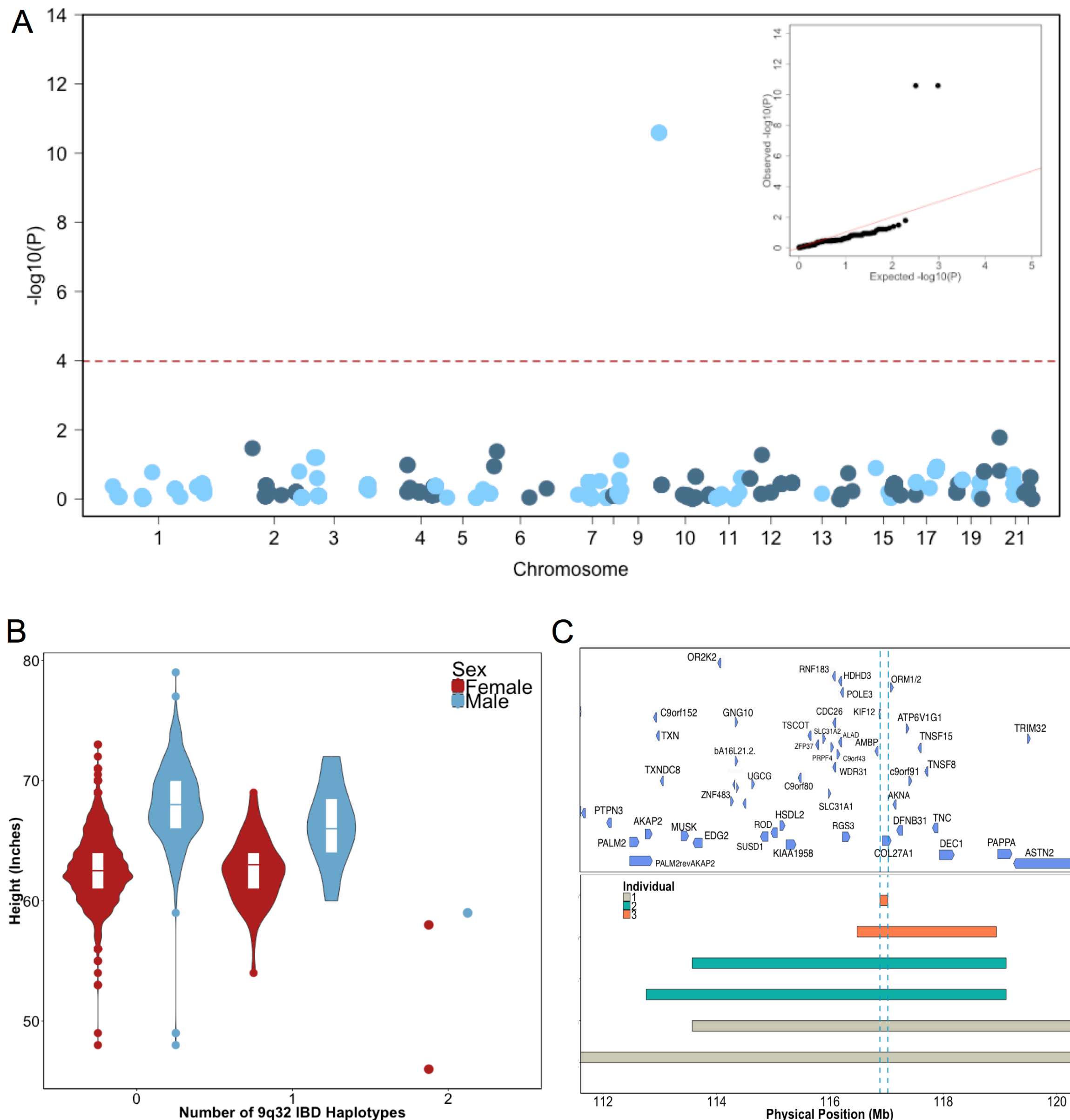

1219
1220 **Figure 2** (A) Identity-By-Descent (IBD) mapping for height in Bio*Me* Puerto Ricans
1221 using a recessive model. Analysis was restricted to IBD-cliques where at least three
1222 individuals were homozygous. Only one IBD-clique achieved Bonferonni significance (at
1223 9q32). (B) Distribution of height among Puerto Rican individuals who carry either 0,1 or
1224 2 copies of the IBD-haplotype reveals a large recessive effect. Homozygous individuals
1225 (those carrying 2 copies of the IBD-haplotype) are on average 6-10" shorter than the
1226 population mean for Puerto Rican ancestry individuals. (C) The minimum shared

bioRxiv preprint doi: https://doi.org/10.1101/141820; this version posted May 24, 2017. The copyright holder for this preprint (which was not certified by peer review) is the author/funder, who has granted bioRxiv a license to display the preprint in perpetuity. It is made available under aCC-BY-ND 4.0 International license.

1227 boundary of the significant IBD-haplotype between the three homozygous individuals
1228 (represented by the dashed blue line). The top panel depicts known genes at the 9q32
1229 locus. The minimum shared boundary of the IBD overlaps the gene *COL2*
1230
1231

bioRxiv preprint doi: https://doi.org/10.1101/141820; this version posted May 24, 2017. The copyright holder for this preprint (which was not certified by peer review) is the author/funder, who has granted bioRxiv a license to display the preprint in perpetuity. It is made available under aCC-BY-ND 4.0 International license.

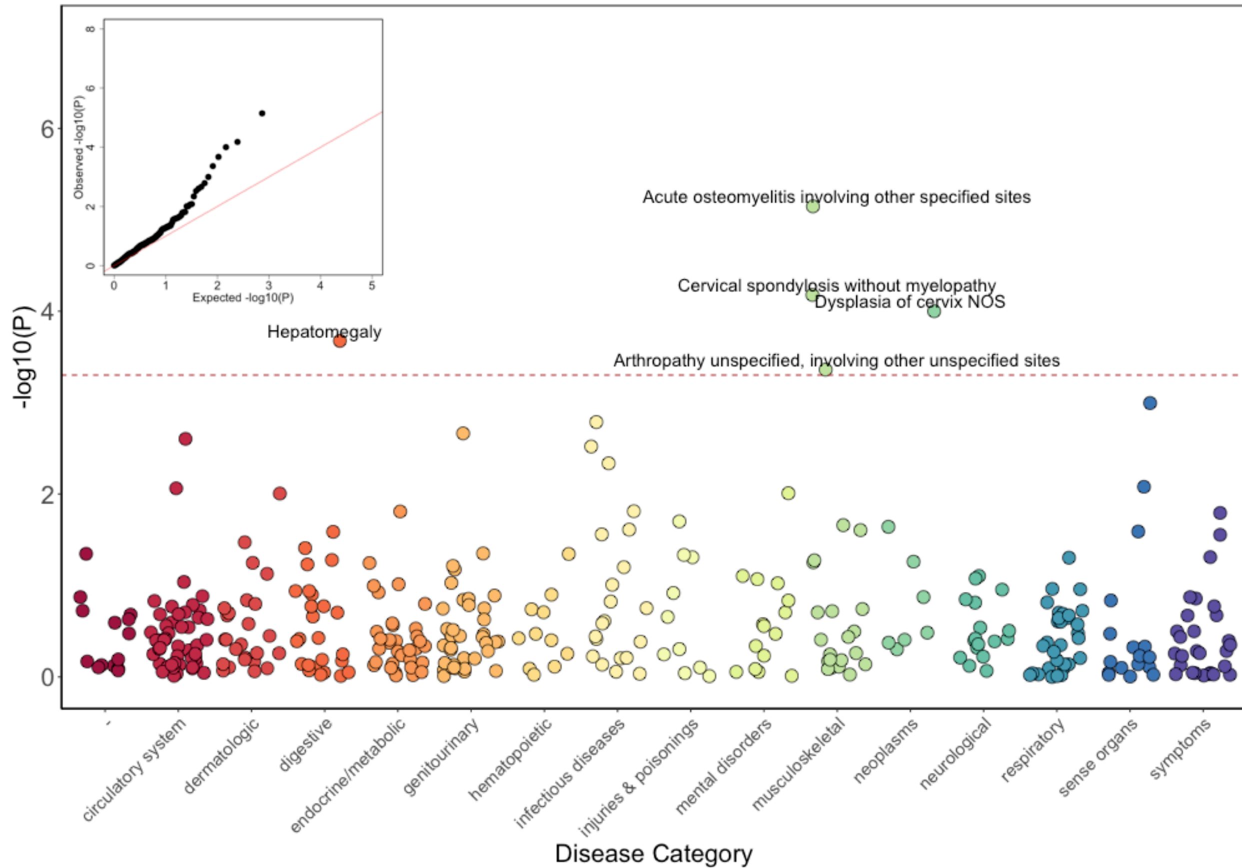

1232

1233 **Figure 3** Phenome-Wide Association Study (PheWAS) of *COL27A1*.pG697R carriers vs

1234 ICD9 billing codes derived from the Electronic Health Records (EHR) under a general

1235 linear model (GLM). Five billing codes achieve significance (FDR adjusted $p<0.05$).

1236 Three of the five significant ICD9 codes are in category of musculoskeletal disorders.

1237

1238

bioRxiv preprint doi: https://doi.org/10.1101/141820; this version posted May 24, 2017. The copyright holder for this preprint (which was not certified by peer review) is the author/funder, who has granted bioRxiv a license to display the preprint in perpetuity. It is made available under aCC-BY-ND 4.0 International license.

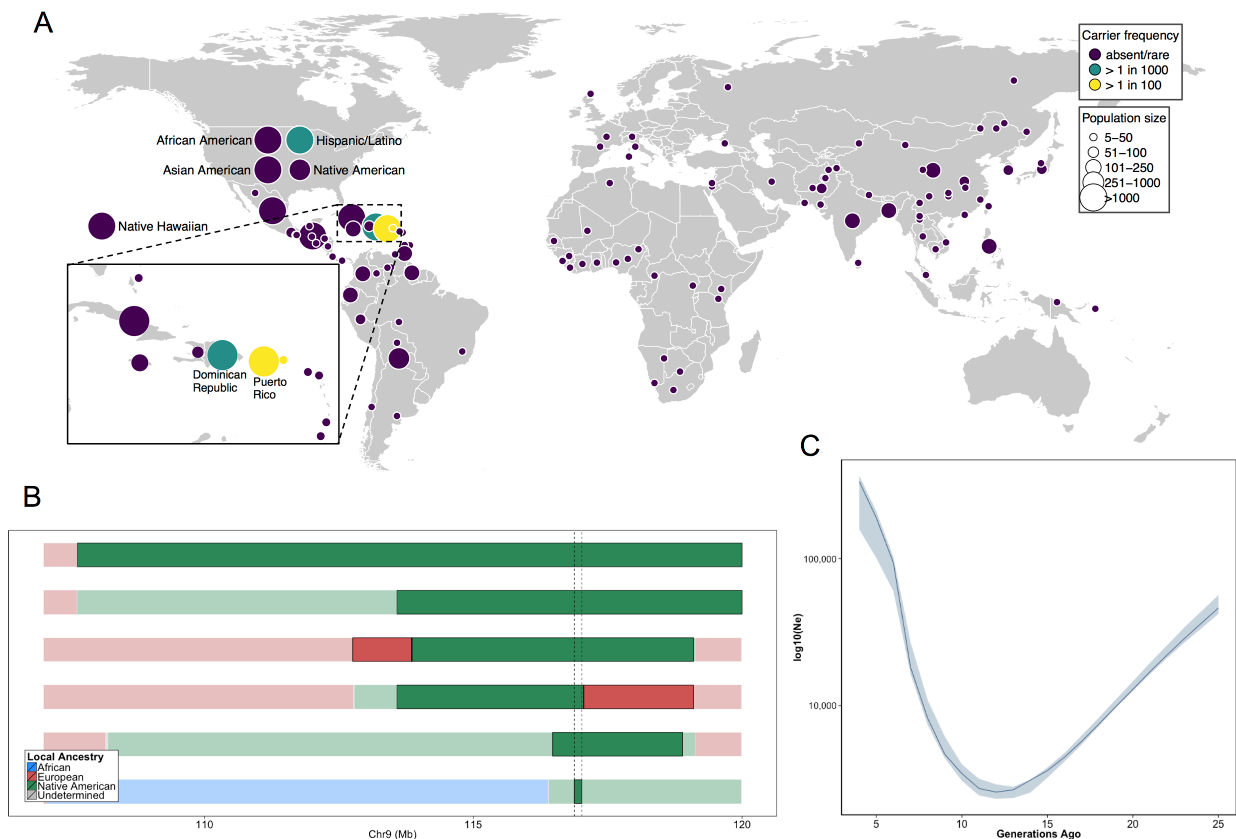

1239

1240 **Figure 4.** (A) Global carrier frequency of *COL27A1*.pG697R in a multi-ethnic database
1241 of over 57,000 individuals representing 112 populations. The variant is absent or very
1242 rare in most populations (purple), at 1:746 and 1:346 carrier frequency amongst
1243 individuals from the Dominican Republic and Hispanic/Latino's in the United States
1244 (green), and at 1:51 and 1:9 carrier frequency amongst individuals from Puerto Rico and
1245 St. Thomas (yellow). (B) Joint analysis of identity-by-descent and local ancestry
1246 haplotypes in three individuals homozygous for the *COL27A1*.pG697R variant. A large
1247 15cM interval on chromosome 9 is shown with local ancestry inferred as African (blue),
1248 European (red) and Native American (green), with shading to indicating the boundaries
1249 of the IBD haplotypes. The location of *COL27A1* is indicated by the dashed line (C)
1250 Effective population size of the Puerto Rican discovery population (N=2816) over the
1251 past 4-25 generations inferred from the tract length distribution of IBD haplotypes

bioRxiv preprint doi: https://doi.org/10.1101/141820; this version posted May 24, 2017. The copyright holder for this preprint (which was not certified by peer review) is the author/funder, who has granted bioRxiv a license to display the preprint in perpetuity. It is made available under aCC-BY-ND 4.0 International license.

1252 suggests that the ancestral population underwent a bottleneck approximately 9-14
1253 generations ago. 95% confidence intervals are represented by blue ribbon
1254